Multi-wavelength variability and quasi-periodic oscillations in Blazars

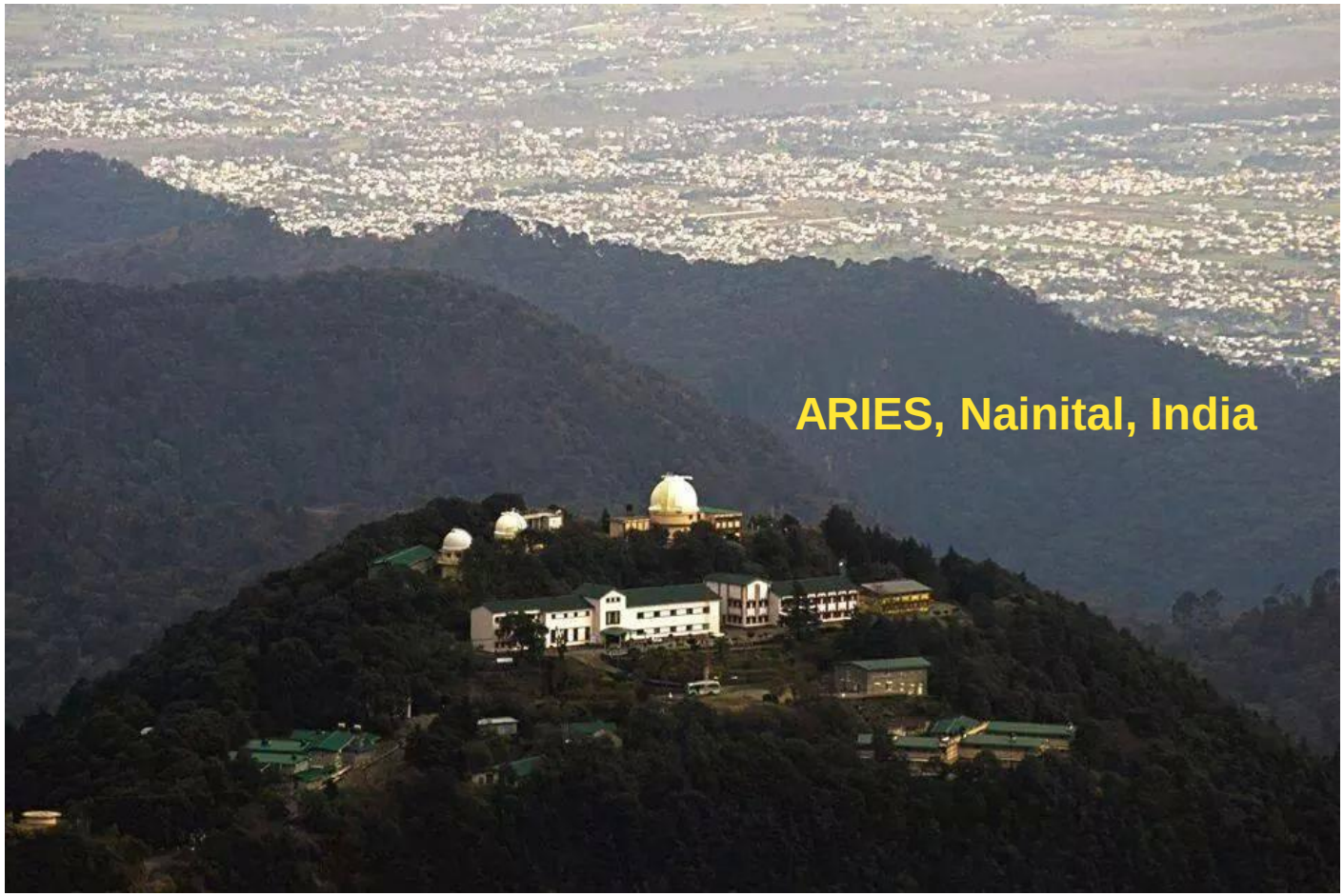

Alok C. Gupta, ARIES, India
alok@aries.res.in, acgupta30@gmail.com

Talk Outline

- Introduction
- Blazars Data and Analysis Tools
- Results

  1. Single and Multi-wavelength Variability of Blazars
  2. Multi-wavelength Variability of Blazars with XMM-Newton, Chandra and NuStar
  3. Quasi Periodic Oscillations (QPOs) in Blazars

- Summary

Blazar (A rare but most powerful class of AGN)

Properties

- ➔ subclass of radio-loud AGN
- ➔ BL Lacs (Featureless optical spectra) + FSRQs (prominent emission lines in optical spectra
- ➔ Flux Variability (in complete EM)
- ➔ Variable Polarization radio to optical bands
- ➔ Non-thermal radiation (predominantly)
- ➔ Jet axis angle < 10^0 (Urry & Padovani 1995)

Classification:

- ➔ LBL ↔ RBL (Red ↔ Low Energy ↔ Radio selected)
- ➔ HBL ↔ XBL (Blue ↔ High Energy ↔ X-ray selected)

Spectral Energy Distribution (SED)

SED Peaks

LBL	IR/optical	GeV
HBL	UV/X-rays	TeV

Emission Mechanism

Low Energy ➔ Synchrotron Radiation

High Energy ➔ Inverse Compton (probably)

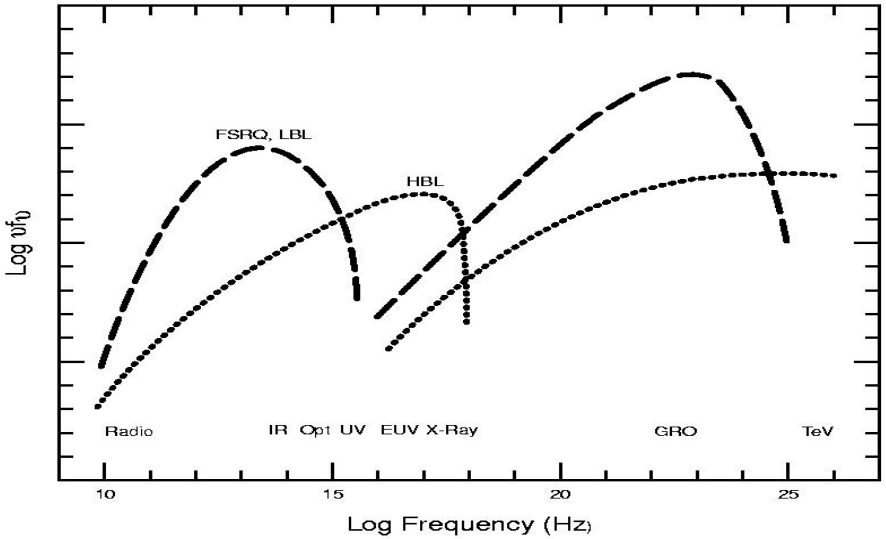

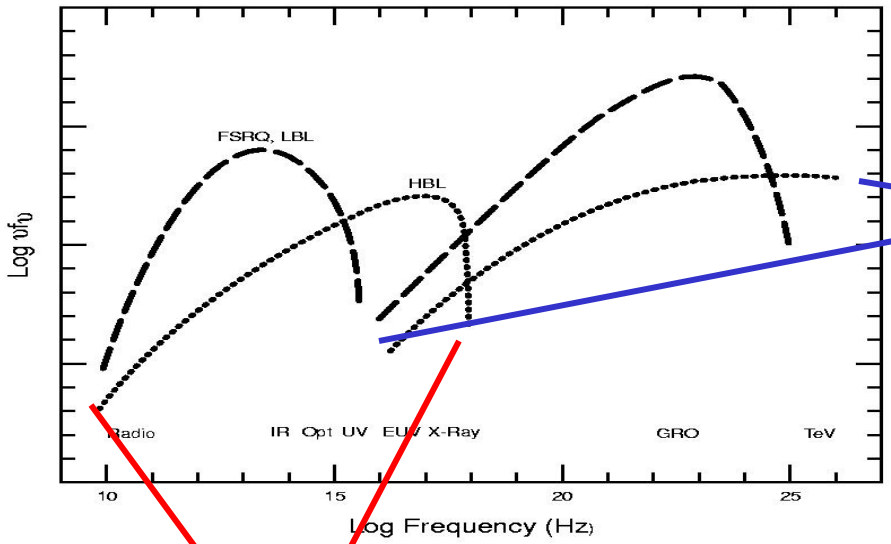

High Energy Part of SED is not well understood. It is usually explained as arising from inverse-Compton (IC) scattering of the same electrons producing the synchrotron emission. These electrons interacts with

1. synchrotron photons → SSC
2. External photons originating in the local environment → EC

Low energy part of SED → well understood

1. Non-thermal Radiation in High State
2. Thermal + Non-thermal Radiation in Low State

Alternative Hadronic Models where Gamma-rays are produced by high energy proton either via proton synchrotron radiation or via secondary emission from photo-pion and photo-pair-production

A lot of challenges to understand high energy part of SED of BLAZARS which can be better understood with multi-wavelength facilities.

Why to Study Blazars?

Blazars are multi-wavelength, and multi-time scale phenomena

Intraday (IDV) – several minutes to less than a day

Short term (STV) – few days to few months

Long term (LTV) – few months to several years

What are the sources of Variability?

Intrinsic

- Shock fronts in the jets (IDV and STV)
- Instabilities or hot spots on the accretion disk (variability in the Low-state) (IDV and STV)
- Binary Black Hole Model (LTV)

Extrinsic

- Gravitational Micro-lensing (IDV)
- It is due to interstellar scintillation (RISS or DISS) and only relevant in low-frequency radio observations. In interstellar scintillation, observed variability crosses the brightness temperature limit 10^{12} K (Compton Catastrophe limit)

Blazar Variability Properties, Time Scales and Physical Implications

Properties	Time Scale	Physical Implications
Irregular & Non-periodic	Few minutes to less than a day (micro or intra-night or intra-day) (IDV)	Size of emitting region, BH mass estimation
Irregular & Non Periodic	One Day to several weeks (short term) (STV)	Useful to search for color variations
Quasi-Periodic	Few months to several years (long term) (LTV)	Useful to predict next Outburst Time, Search for time lag in different energy bands.

Simultaneous multi-wavelength observations of a particular blazar is extremely useful to understand the emission mechanism of blazars and emitting regions in different energy bands.

Hot Spot on/above Accretion Disk

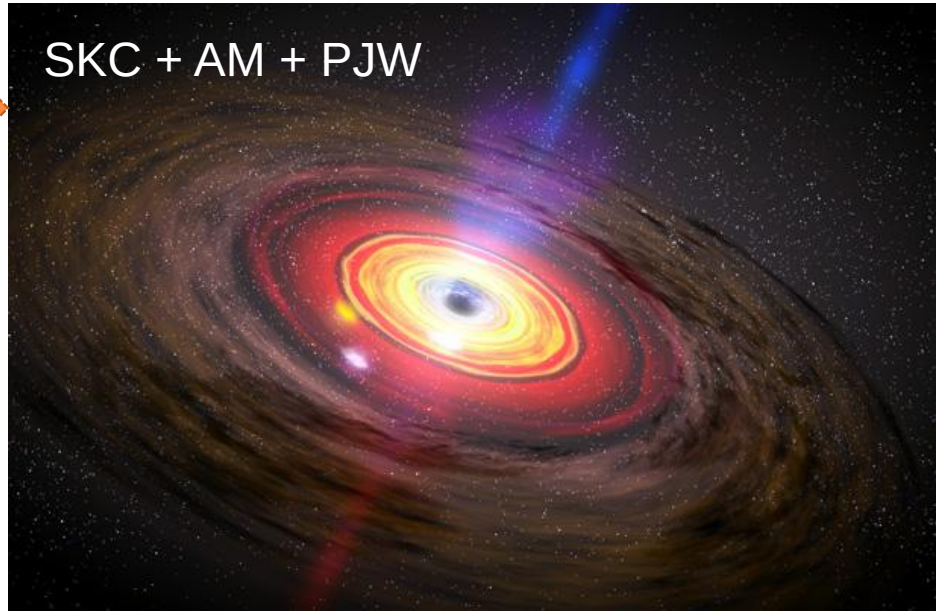

Helical Jet Structure Model

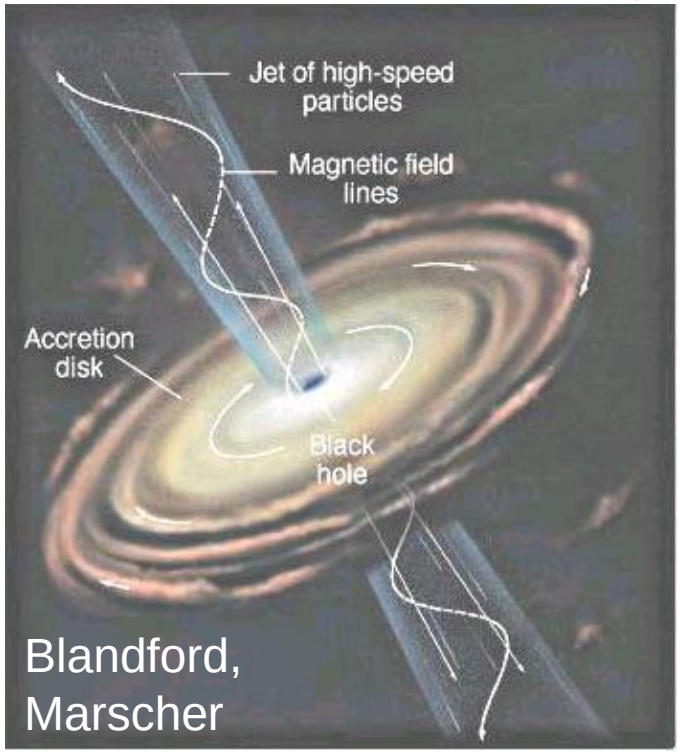

Binary Black Hole Model

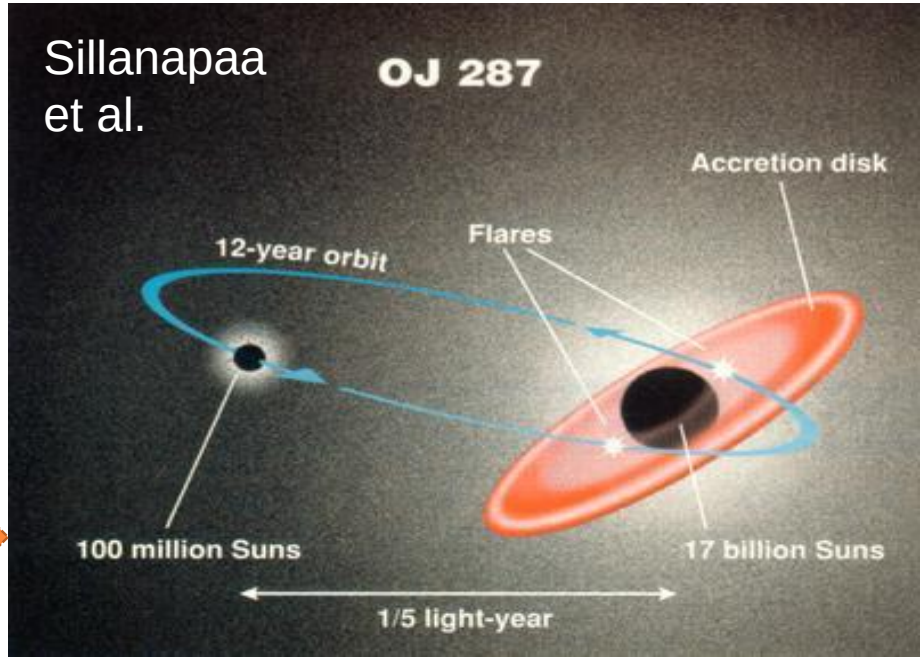

Project 1.

Single and Multi-wavelength Variability of Blazars

IDVs in LBLs

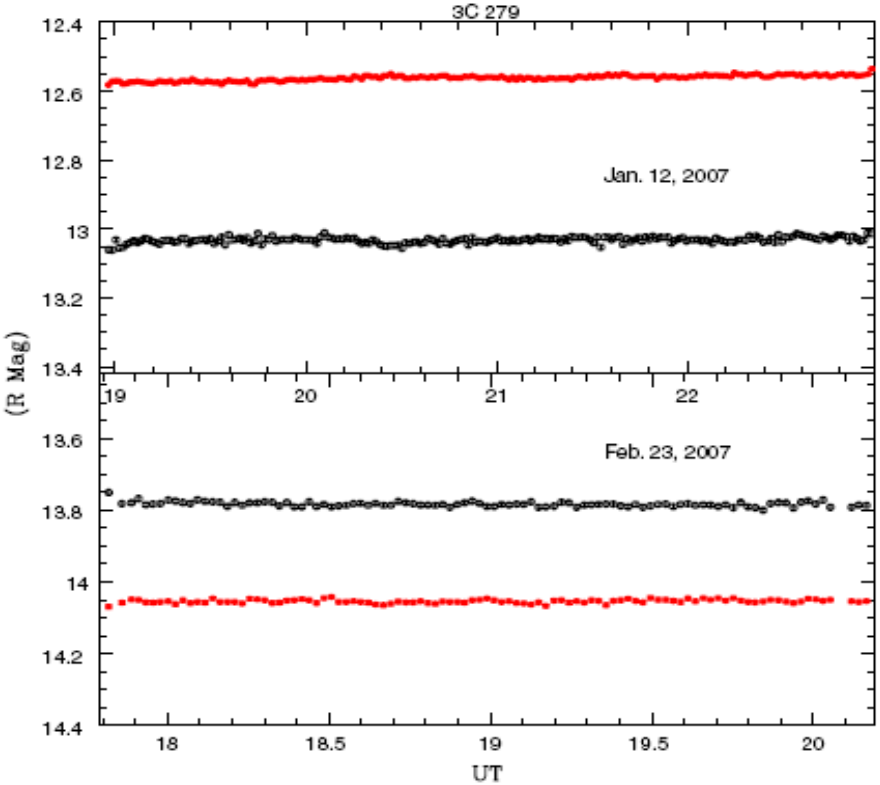

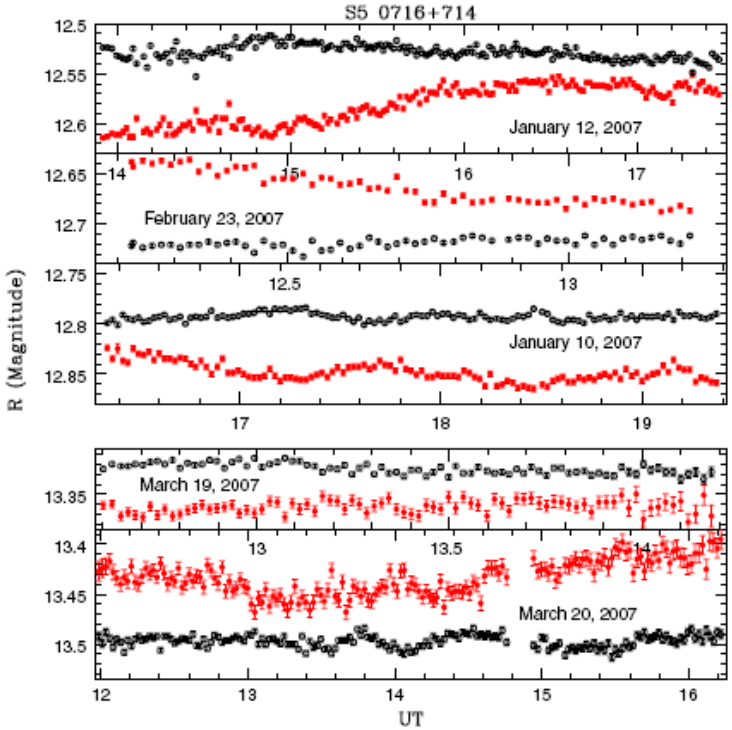

No IDV detection in the blazars due to uniform jet emission.

Detected variability in flux measurement on IDV timescales are due to irregularities in jet flow

Gupta et al. 2008, AJ, 135, 1384

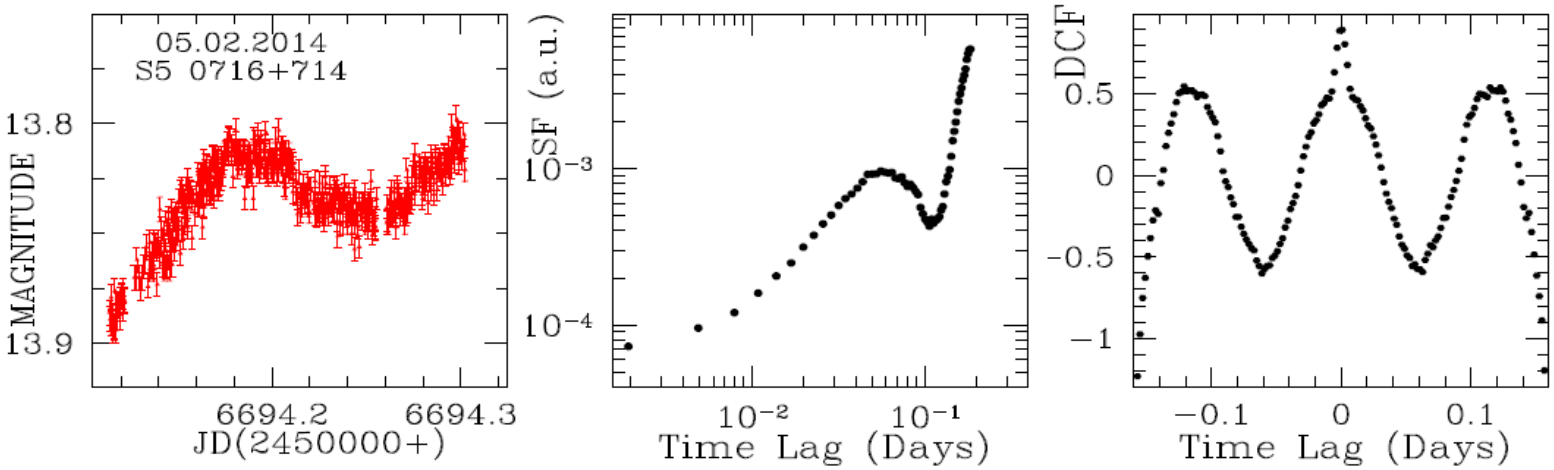

Figure 7. *R*-band optical IDV LC of the blazar S5 0716+714 and their respective SFs and DCFs. The remainder of these observations and analyses are presented as online-only material.

IDV timescale is used to get the upper limit of M_BH for S5 0716+714. We got 1.74 * 10^8 M_sun.

Agarwal, Gupta et al. 2016, MNRAS, 455, 680

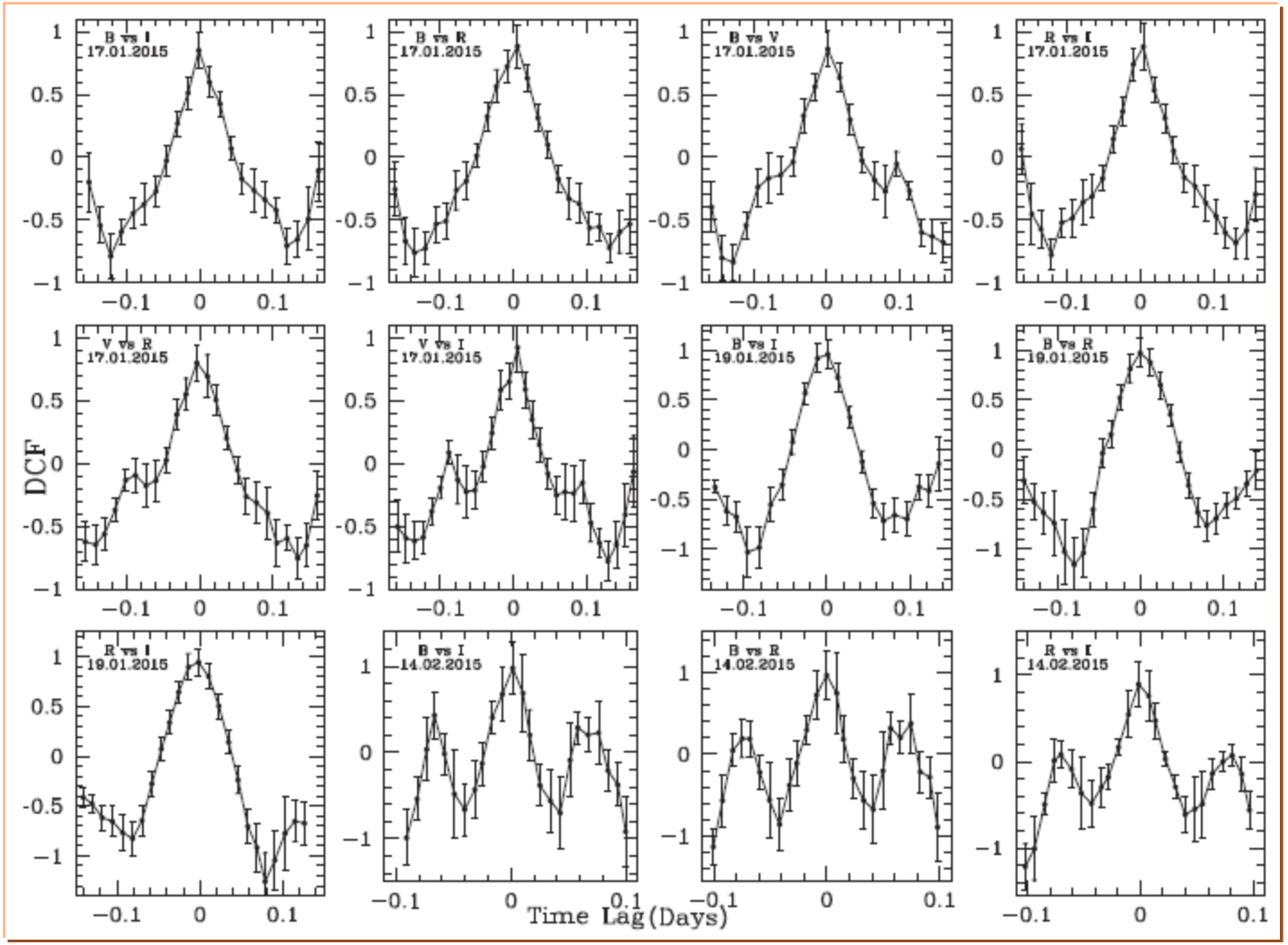

S5 0716+714

On IDV timescale, we found optical bands are well correlated with zero lag. It gives evidence of co-spatial origin of emission in all optical bands.

Agarwal, Gupta, et al. 2016, MNRAS, 455, 680

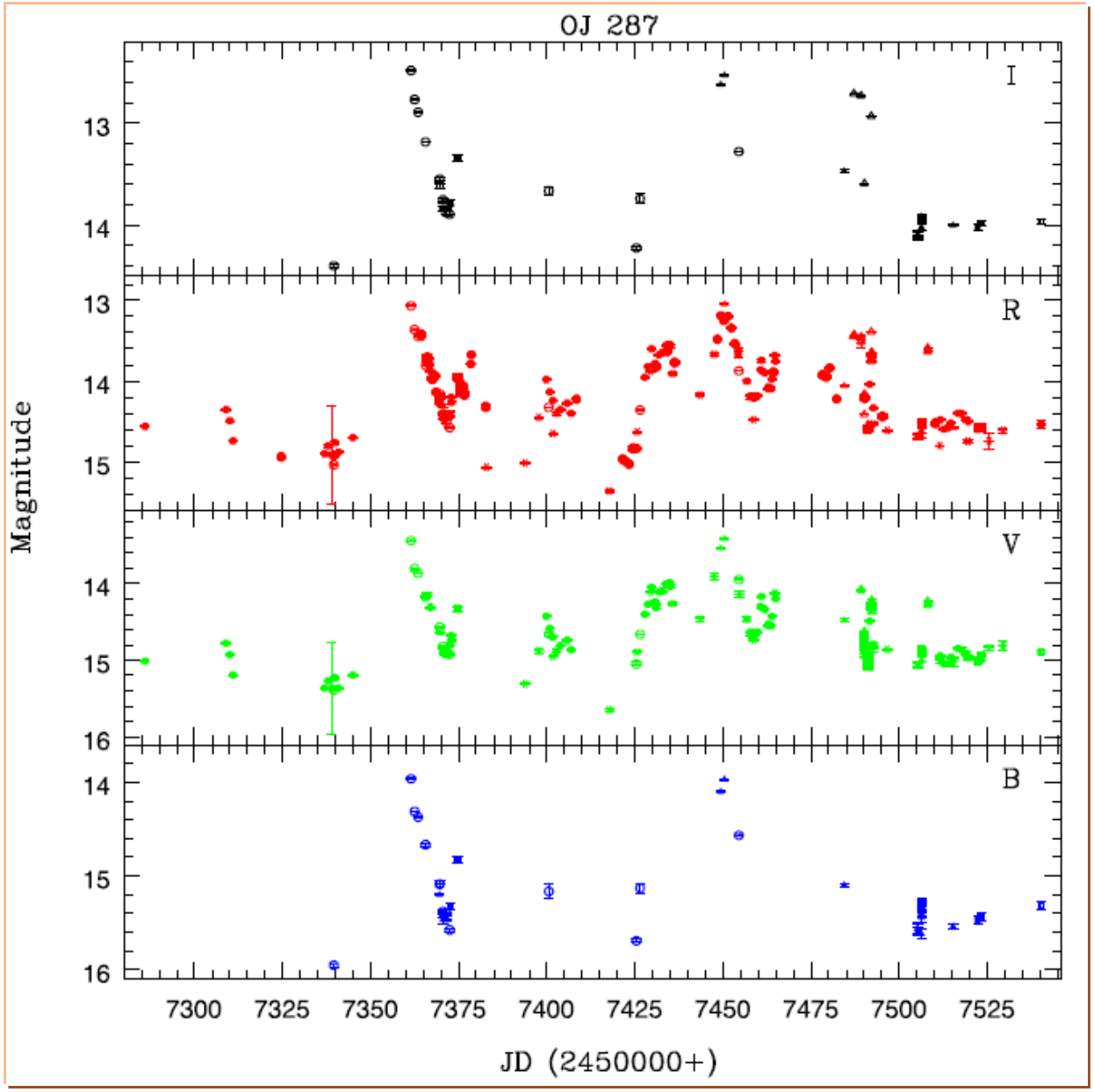

STV in LBLs

Observations are carried out during September 2015 – May 2016 by using 9 optical telescopes world wide.

We detected IDV, STV and color variation on STV timescales.

We also detected multiple flaring events in our observations.

Gupta et al. 2017, MNRAS, 465, 4423

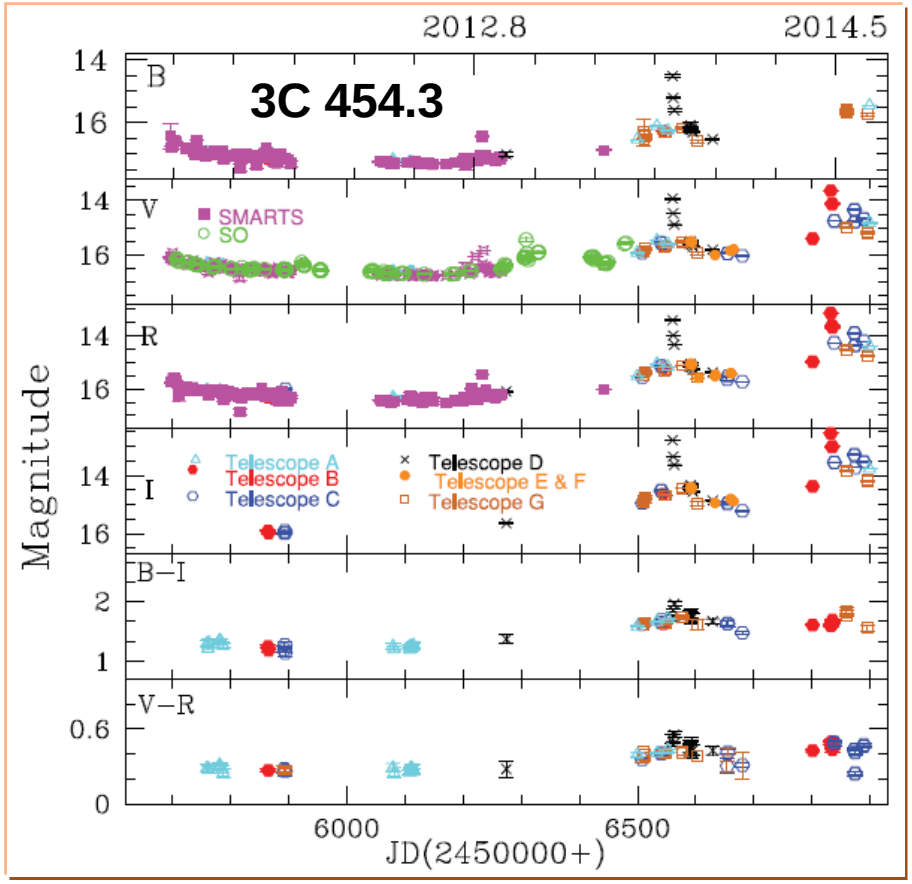

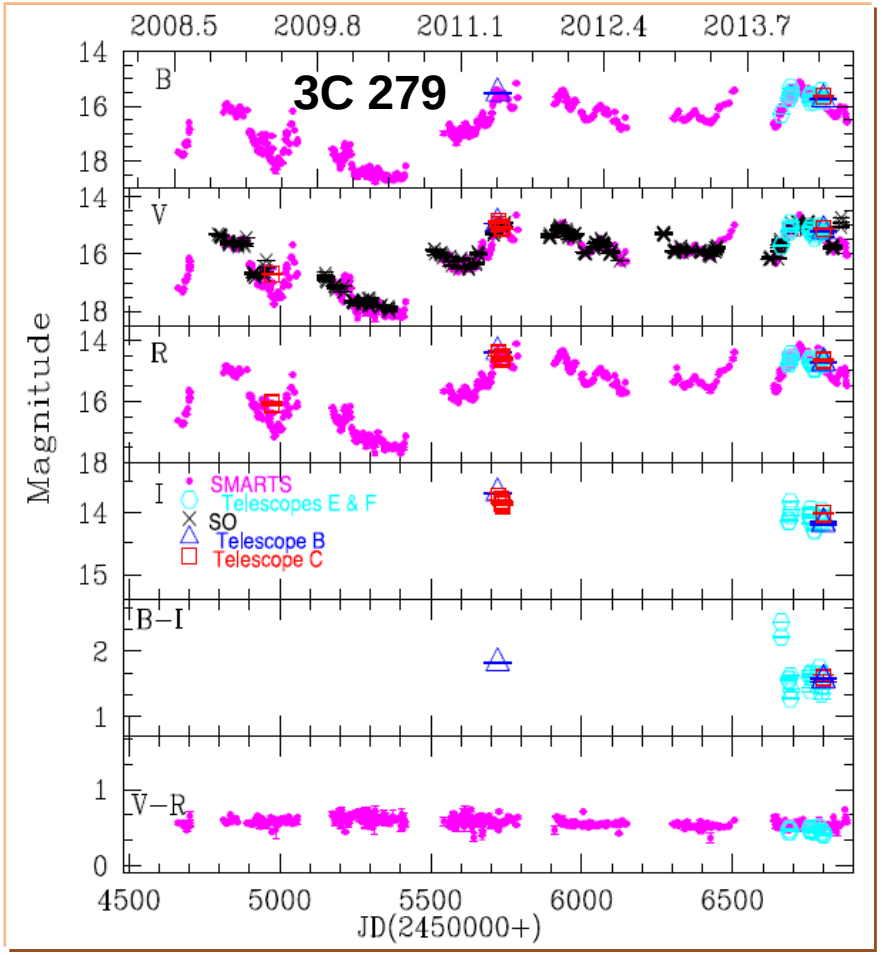

Optical LTV Results: We noticed large amplitude optical LTV in flux in almost in all blazars, we observed.

In general BL Lac objects show BWB while FSRQs show RWB trend on STV and LTV timescales. It gives a signature of thermal emission from accretion disk in addition to non-thermal jet emission.

Agarwal, Gupta et al. 2016, MNRAS, 455, 680

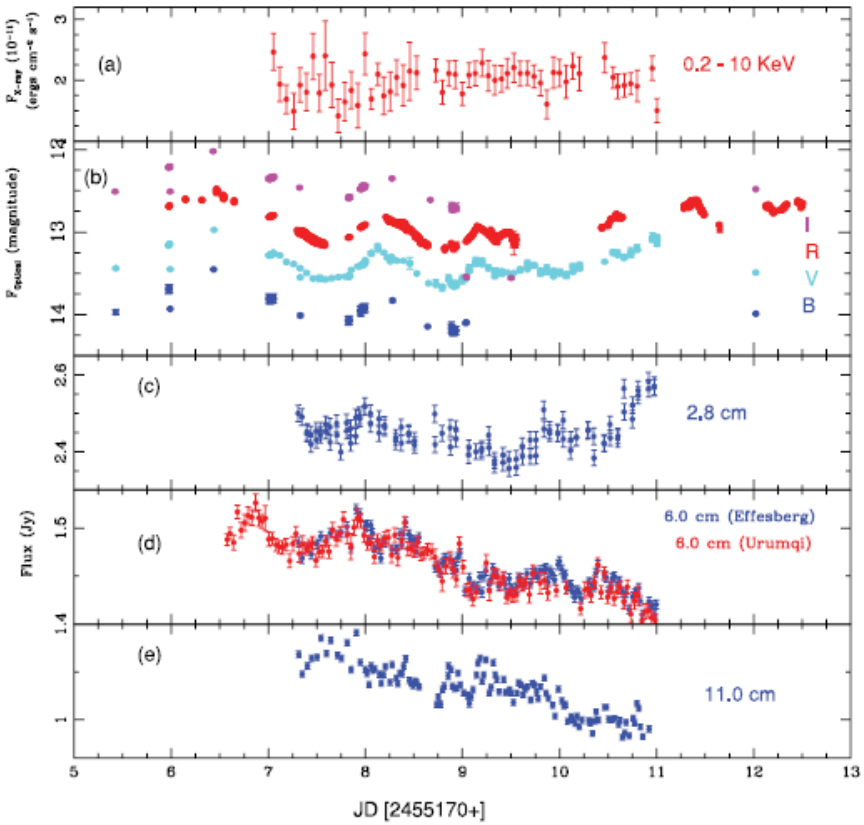

Simultaneous multi-wavelength observations of 0716+714 during Dec 11-15, 2009 (core campaign period).

IDV detected in radio and optical bands.

Total change in optical bands ~ 0.8 mag.

Correlated variability is found in different optical bands.

2.8 cm band data leads 6 and 11 cm bands.

SED was constructed with non simultaneous Fermi data and we got Doppler factor ≥ 12 – 26 which is relatively high for a BL Lac.

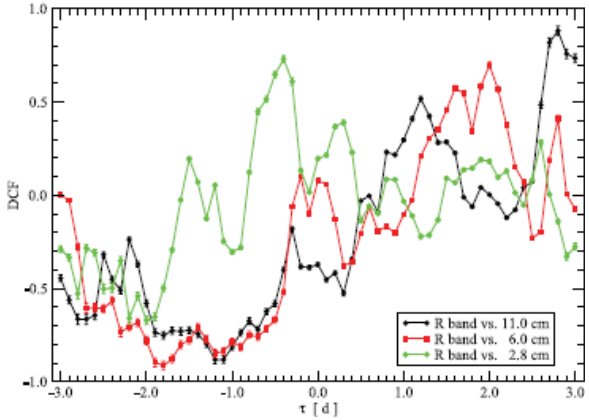

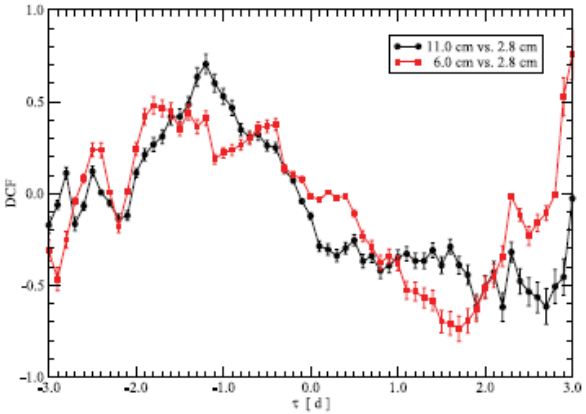

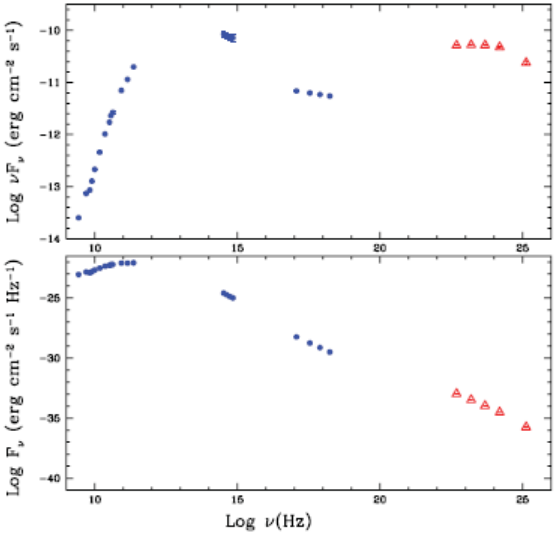

Gupta et al. 2012, MNRAS, **425**, 1357

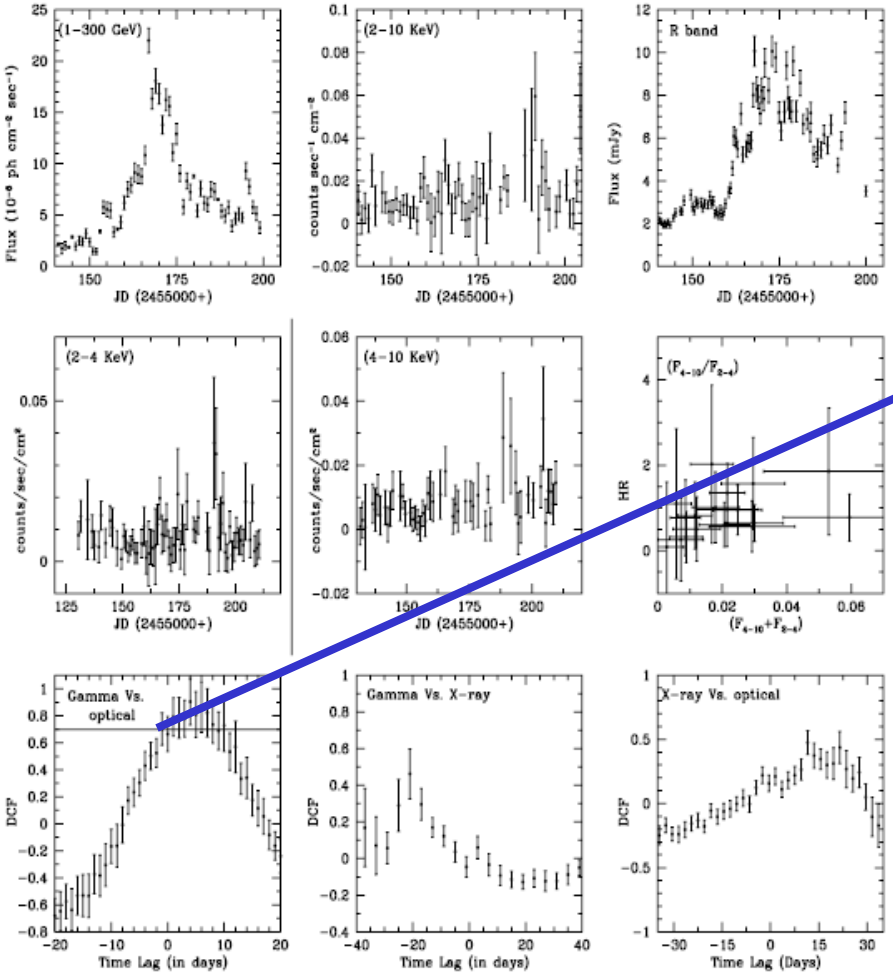

Figure 7. Gamma, X-ray, and optical LCs of 3C 454.3 (upper panels); X-ray LCs for 3C 454.3 in 2–4 keV, 4–10 keV and hardness intensity plot (middle panels); DCF between gamma vs. optical (horizontal line indicates 99% significance level), γ-ray vs. X-ray, and X-ray vs. optical (in lower panels).

3C 454.3

99.9% significance level by using MC simulation.

In the blazar 3C 454.3, we got strong optical and Gamma-ray correlations with time lag of ~ 4 days (gamma-ray leading optical).

External Compton emission mechanism can explain the findings.

Gaur, **Gupta** & Wiita, 2012a, AJ, 143, 23

Optical Flux and Polarization Observations of BL Lacertae during 2008 - 2010

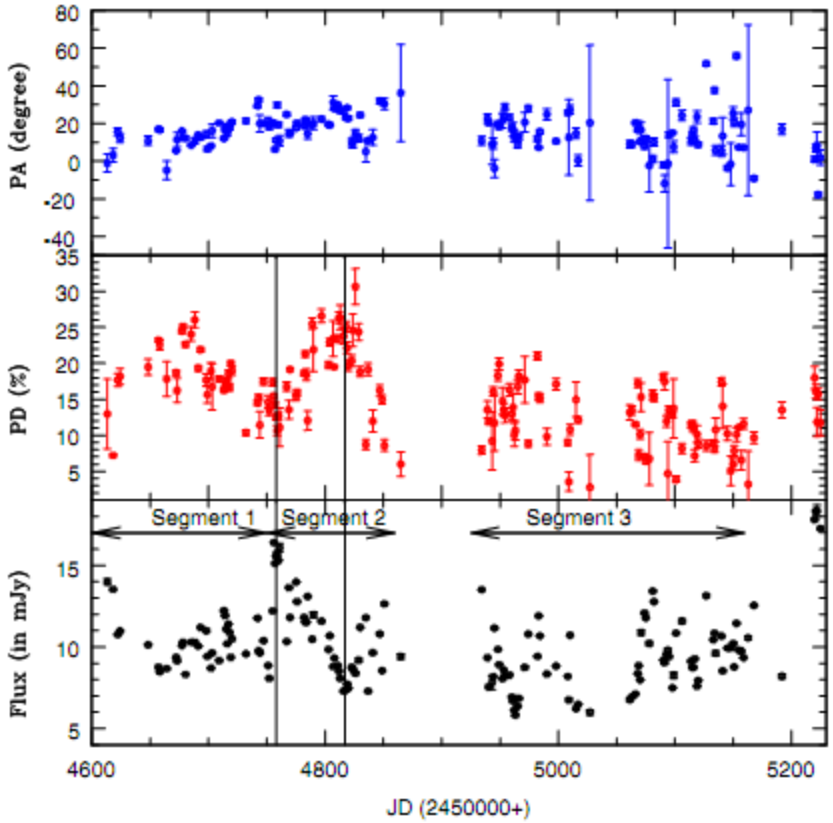

Figure 1. *V* passband light curve of the BL Lac over the two observing seasons during the period May 2008–Jan 2010 from KANATA telescope (lower panel), its percentage polarization (middle panel), and polarization angle (in upper panel). Segments 1, 2, and 3 are marked in the bottom panel of the figure.

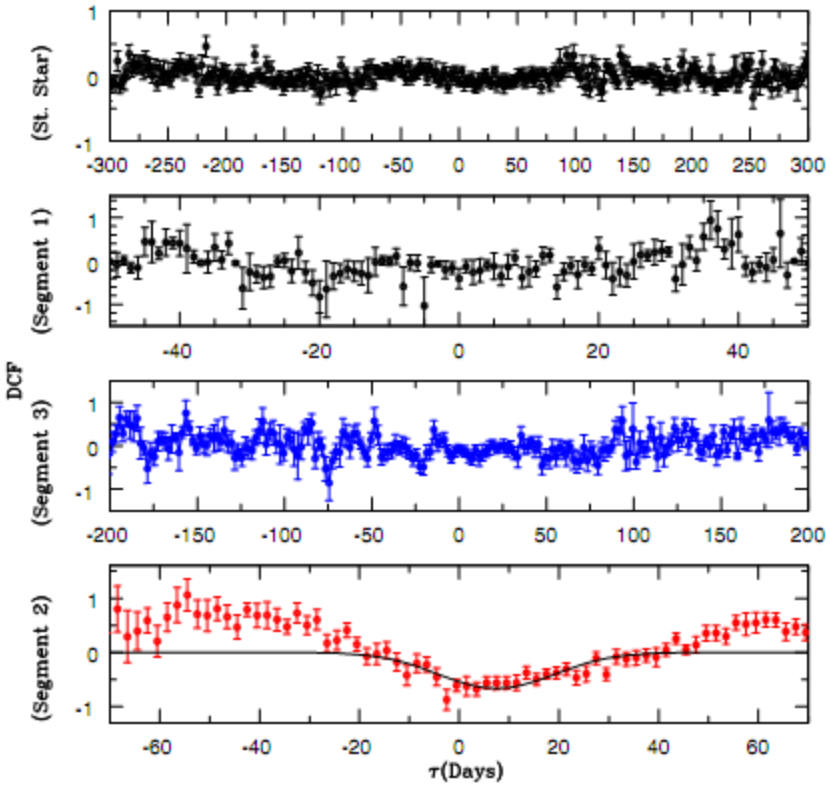

Figure 2. DCF for an unpolarized standard star is shown in the top panel. The DCF between optical flux and polarization degree for the portions of the observations presented and marked in Figure 1 as Segment 1, Segment 3, and Segment 2 are shown moving downward; the solid line represents the fitted Gaussian function in Segment 2.

Anti-correlated optical flux and polarization is unique result and possibly detected for the first time in BL Lacertae.

Gaur, Gupta, et al. 2014, ApJ Letters, 781, L4

The result is consistent with a model with at least two emission regions being present, with the more variable component having a polarization direction nearly perpendicular to that of the relatively quiescent region so that a rising flux can produce a decline degree of polarization.

We used the more generalized recent model by Larionov et al. (2013), where small variation in Lorentz factor by keeping other parameters e.g. viewing angle, evolution of outburst, spectral index, shock plasma compression ratio, etc. as fixed may show variety of variation in flux and polarization.

Project 2.

Multi-wavelength Variability of Blazars with XMM-Newton, Chandra and NuStar

- Stable Flux
- Decline Flux
- QPO
- Flare

- Stable Flux (1a)
- Decline Flux (1b, 3a)
- QPO (2)
- Flare (1c, 3b)

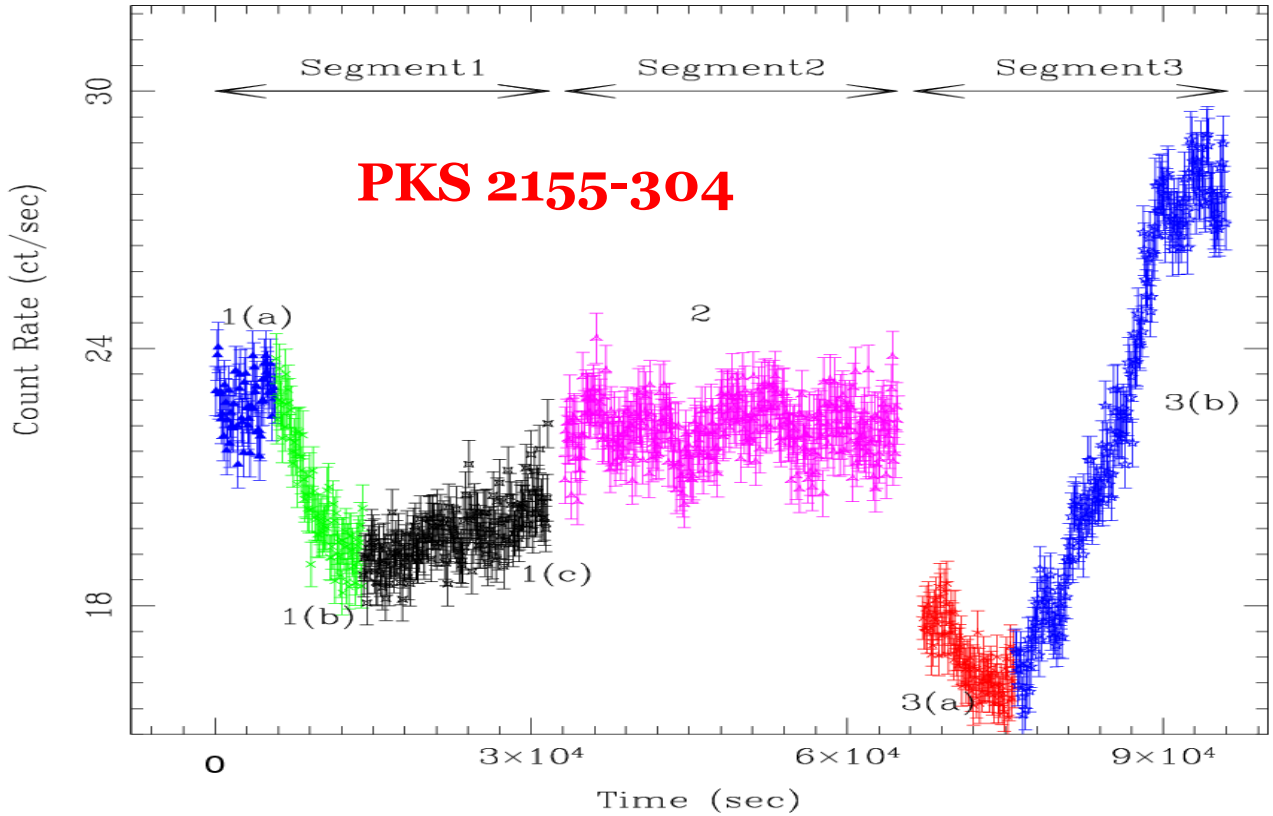

- In sub-segments: 1(a) flux is stable; 1(b) & 3(a) flux decreases; 1(c) & 3(b) show flux rising trend.
- In sub-segment: (2) a hint of weak QPO is detected (Gaur, **Gupta,** et al. 2010, ApJ).
- The percentage variability of segment 1-3 in 0.3 – 10 keV band are 6.6±0.16, 1.5±0.22 and 21±0.15, respectively.

Evidence of jet and accretion disk based models

Bhagwan, **Gupta**, Papadakis, Wiita, 2017

X-ray Variability of the Blazar PKS 2155-304 on IDV Timescale

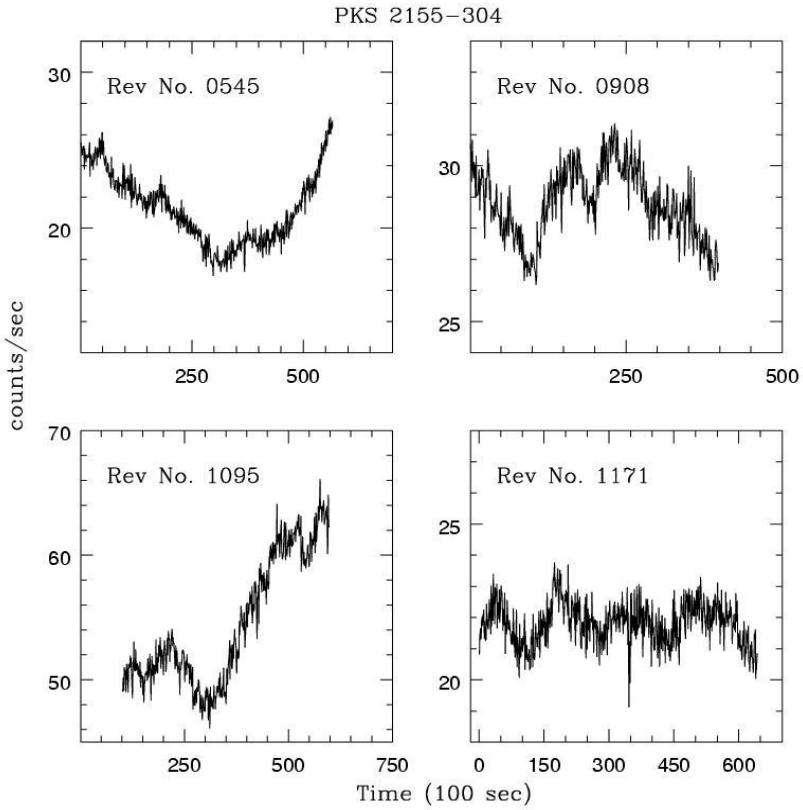

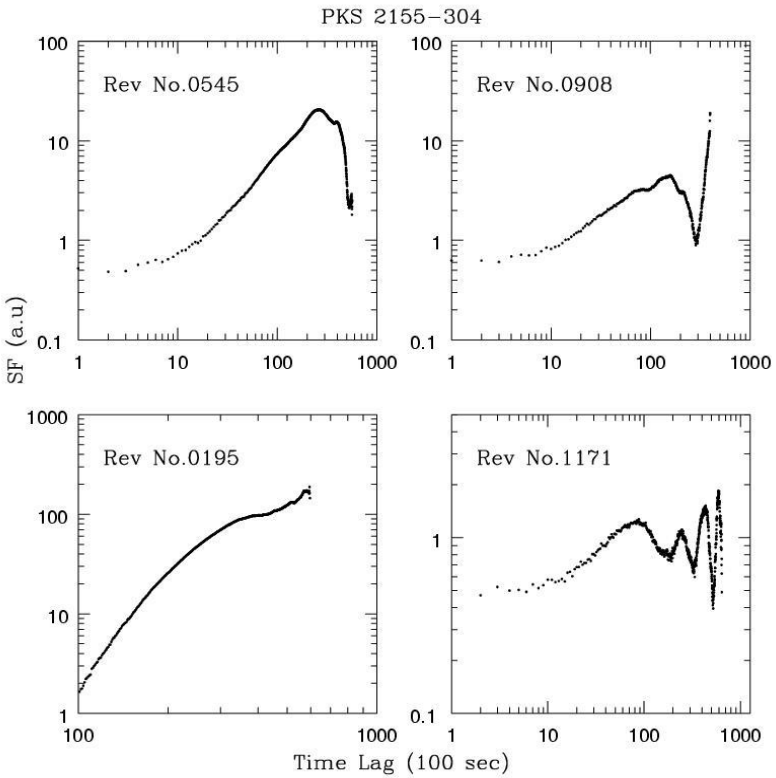

- Out of 14 LCs, only 7 have shown IDV timescales in the range of 15.7 to 41.4 ks.
- On 6 occasions, IDV timescale is longer than the data length.
- Hint of QPO (possible period ~ 5.9 ks) on one occasion.

Evidence of jet and accretion disk based models

Gaur, **Gupta**, Lachowicz, Wiita, 2010, ApJ, 718, 279

Some other examples of IDV of TeV blazars with Chandra and NuStar

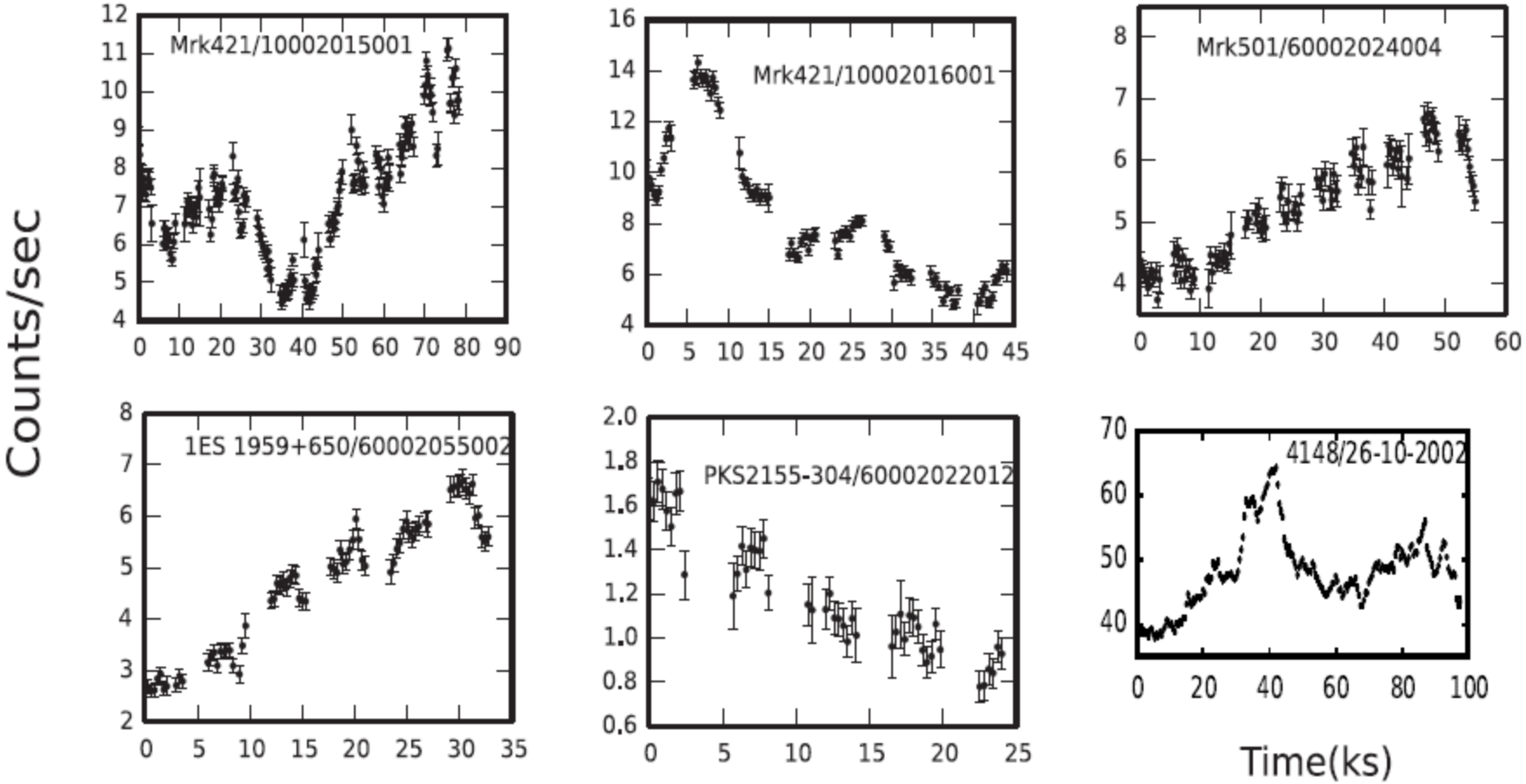

Large amplitude IDV is noticed in TeV blazars observed by NuStar (3 – 79 keV) and Chandra (0.3 – 10 keV).

Evidence of jet and accretion disk based models

Pandey, Gupta, Wiita 2017, 2018, ApJ; Aggrawal, Pandey, Gupta et al. 2018, MNRAS

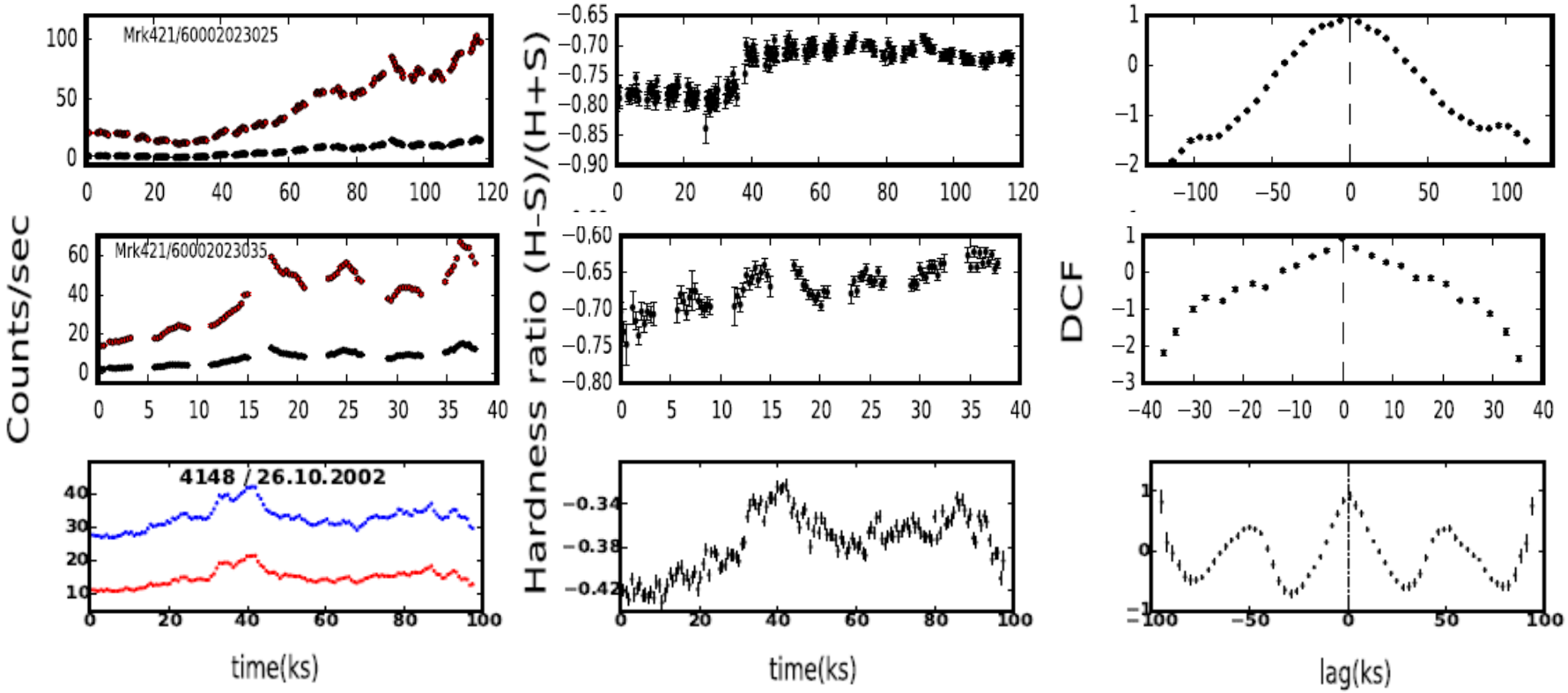

- **In soft (3 – 10 keV) vs hard (10 – 79 keV) using NuStar and soft (0.3 – 2.0 keV and hard (2 – 10 keV) using Chandra, we noticed spectra harden with increasing flux ➔ evidence for harder when brighter.**

- **Soft and hard light curves in NuStar and Chandra are well correlated with zero lag ➔ co spatial emission region by same population of leptons.**

Pandey, Gupta, Wiita 2017, 2018, ApJ; Aggrawal, Pandey, Gupta et al. 2018, MNRAS

Intra-day Variability Timescales of TeV Blazars using NuStar and Chandra

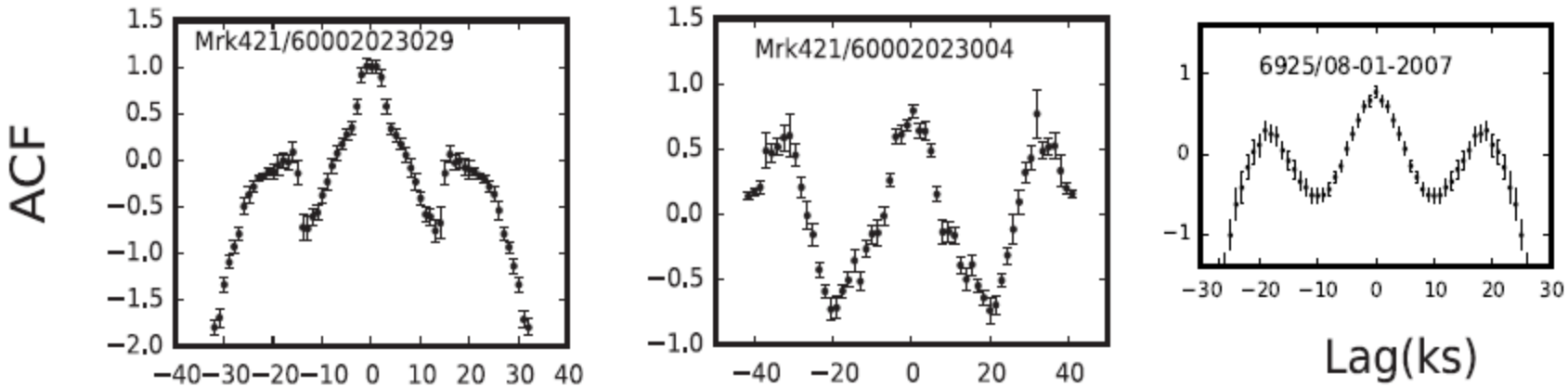

Using intra-day variability timescales, we calculated following parameters of blazars

Model Parameters for *NuSTAR* Blazars

Blazar	t_{var}(s)	δ	B (G)	γ	R (cm)
Mrk 421	2500	25	$\geqslant 0.12$	$\leqslant 9.0 \times 10^5$	$\leqslant 1.8 \times 10^{15}$
Mrk 501	8000	15	$\geqslant 0.07$	$\leqslant 1.5 \times 10^6$	$\leqslant 3.5 \times 10^{15}$
PKS 2155−304	29600	30	$\geqslant 0.02$	$\leqslant 2.0 \times 10^6$	$\leqslant 2.4 \times 10^{16}$

Similar results we found for the Blazar Mrk 421 using Chandra data

Pandey et al. 2017, 2018, ApJ; Aggrawal et al. 2018, MNRAS

Double outburst in Mrk 421 on STV timescale using NuStar

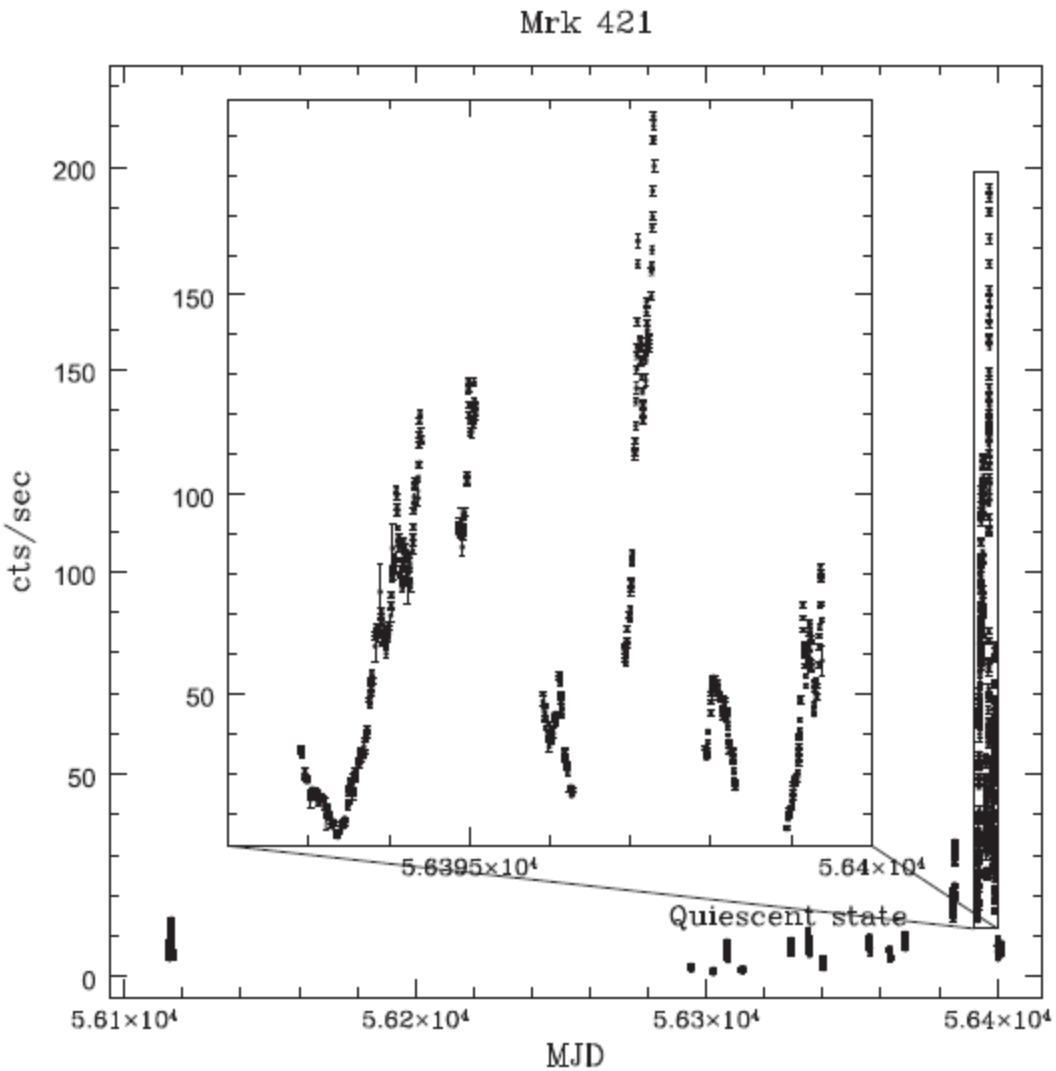

Figure 4. Short-term variability of Mrk 421.

Strong double X-ray outburst is explained by jet – in – jet model

Pandey, Gupta & Wiita, 2017, ApJ, 841, 123

Long Term Variability of 3C 273

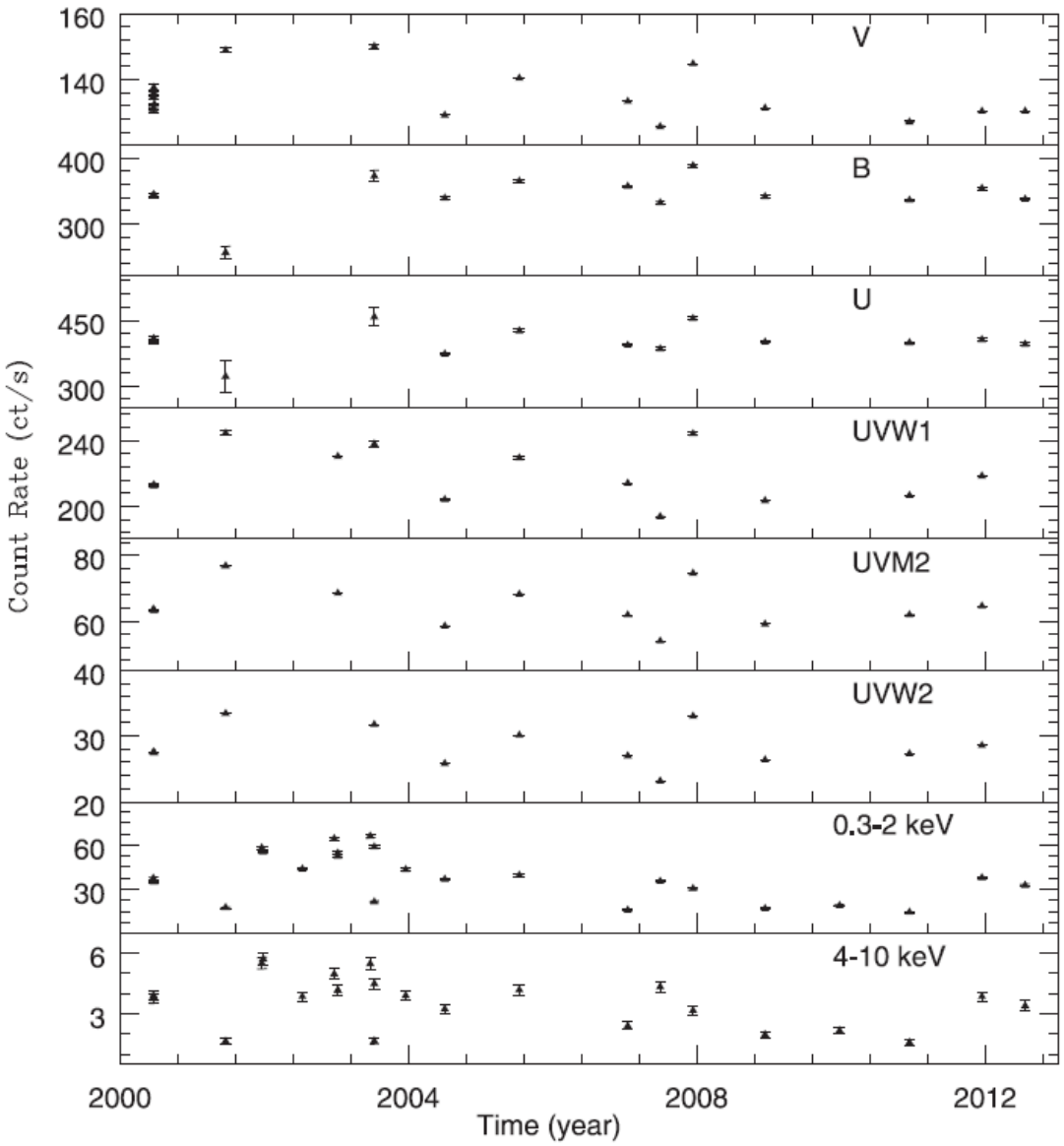

- During the years 2000 – 2012, 3C 273 has 21 observations simultaneously in OM and EPIC-PN.
- We find significant variations, in all bands, on time-scale of years.
- Our visual inspection show that in the long term LCs, optical & UV bands are well correlated and the same is true for hard and soft X-ray bands.

Kalita, **Gupta**, et al., 2015, MNRAS, 451, 1356

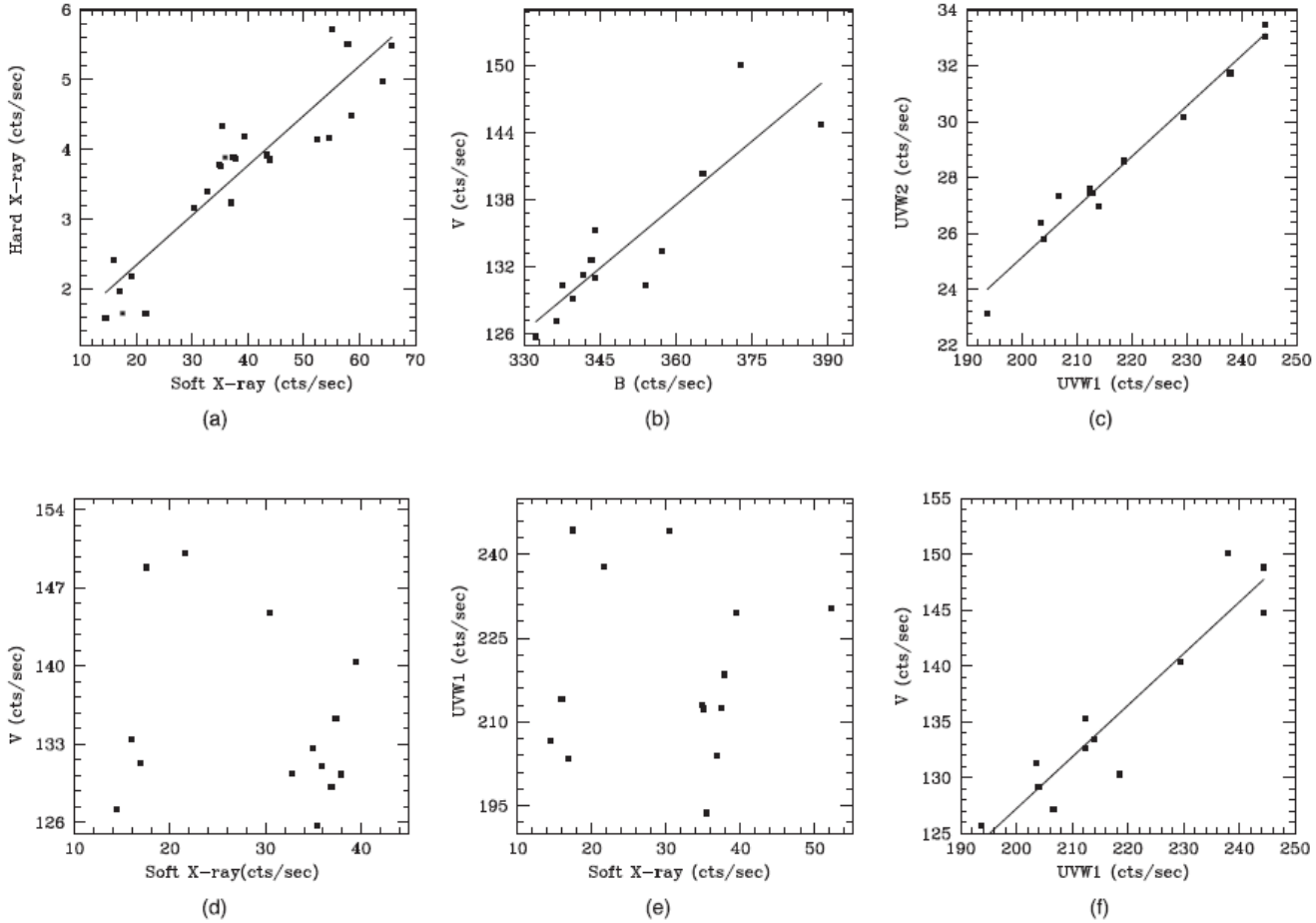

Figure 4. Correlations in variability between different optical, UV and X-ray bands.

Flux Variations in Optical/UV are not correlated with X-rays. But optical/UV bands are well correlated, similarly soft and hard X-ray bands are well correlated ➔ Optical/UV emissions in this blazar may arise from same population of leptons. But X-ray emission is due to a different population of leptons.

Kalita, **Gupta**, et al., 2015, MNRAS, 451, 1356

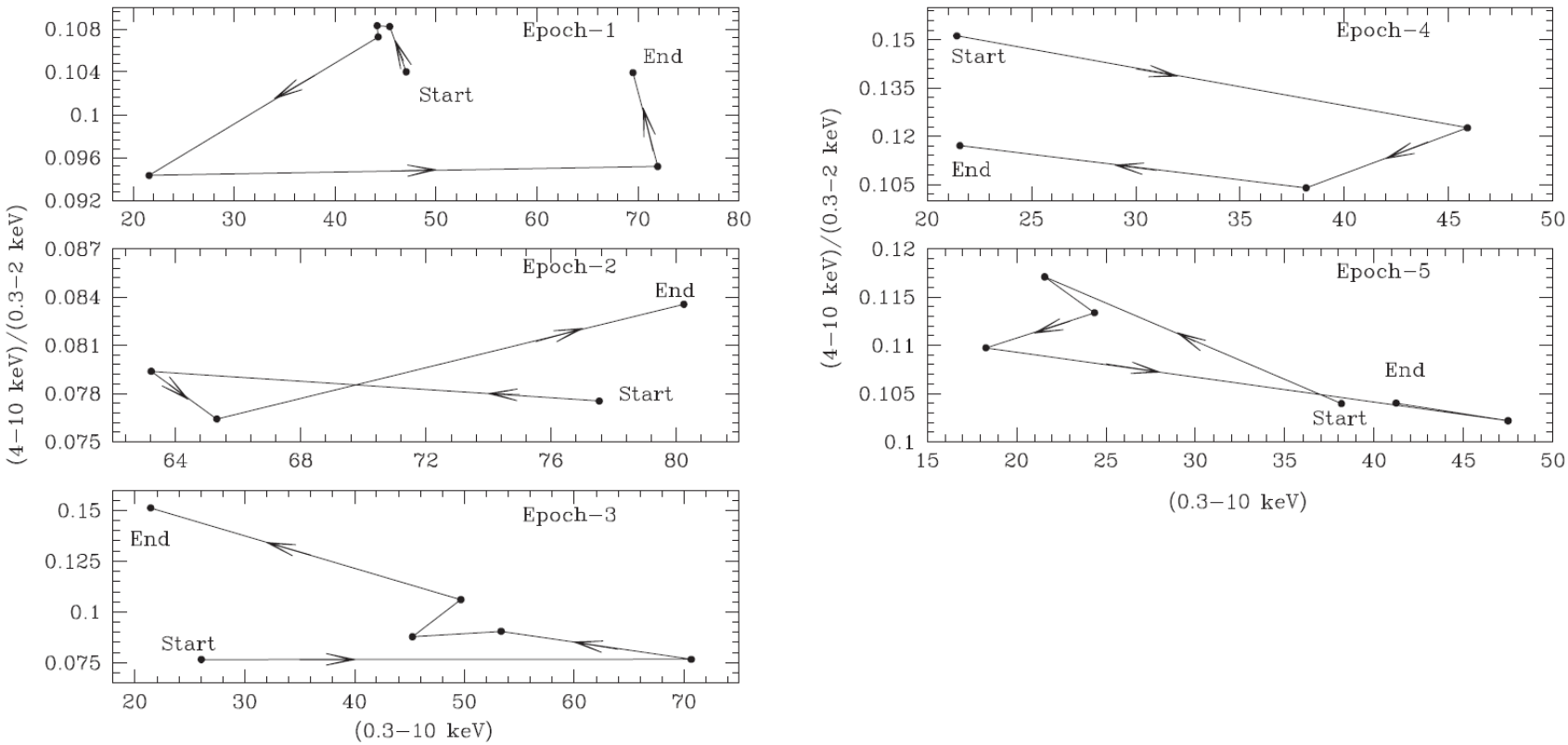

Figure 5. Spectral evolution of 3C 273 in different epochs. Arrows indicate the directions of the loops. Here, the term epoch in the plots represent different time intervals during which the data were acquired for each corresponding loop: Epoch-1 = 13.06.2000–22.12.2001; Epoch-2 = 17.12.2002–18.06.2003; Epoch-3 = 07.07.2003–12.01.2007; Epoch-4 = 12.01.2007– 09.12.2008; Epoch-5 = 06.12.2007–16.07.2012. The clockwise and anti-clockwise loops are distinct and closed or nearly so, presenting a clear evidence of alternate acceleration and cooling mechanism.

In the above HR vs Flux plots, we found clockwise and anti-clockwise loop on different epochs ➔ both synchrotron cooling as well as particle acceleration are at work on different epochs of observations.

Kalita, **Gupta**, et al., 2015, MNRAS, 451, 1356

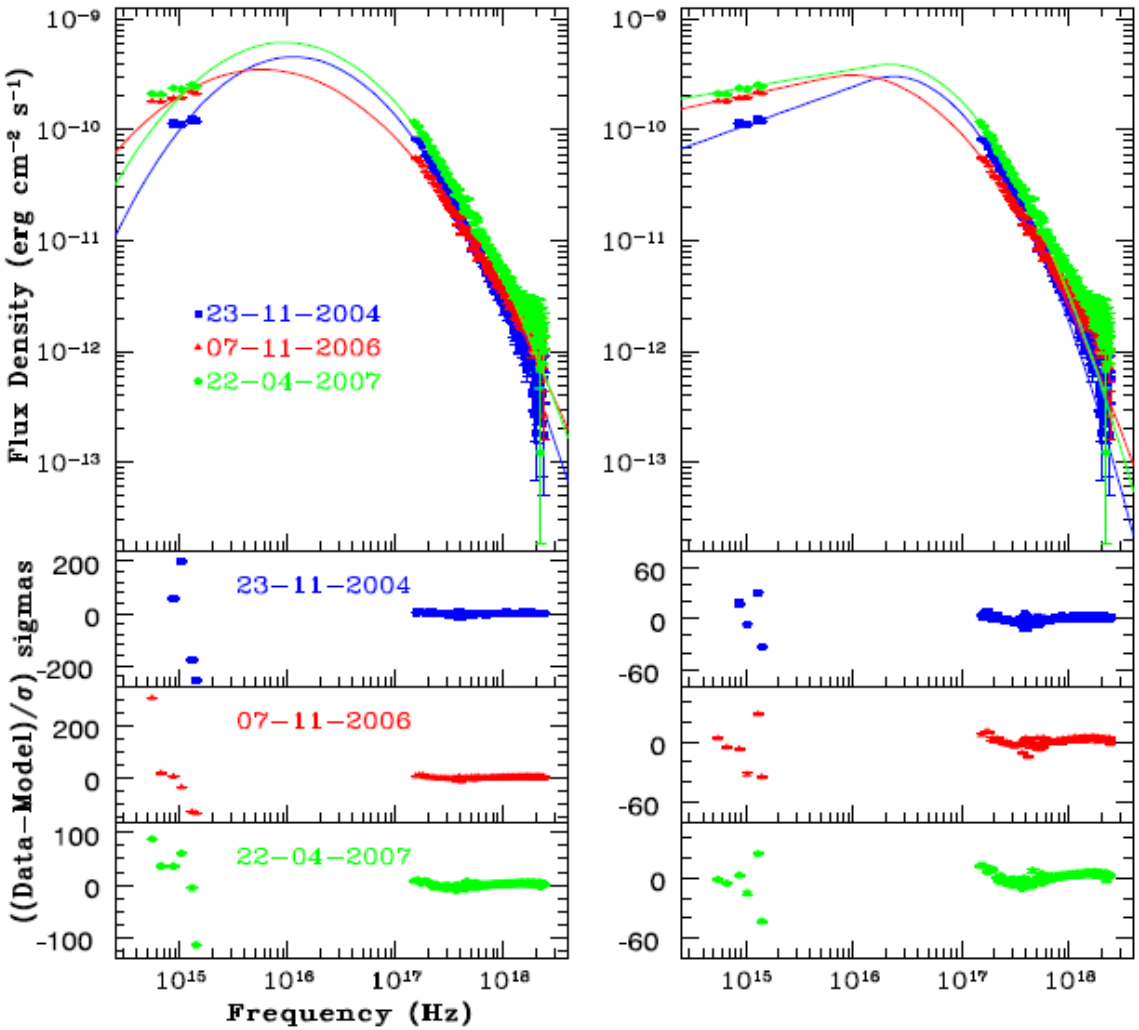

Log Parabolic (LP) Model

Log Parabolic + Power Law (LPPL) Model

- We made the SEDs for all 20 observations which span more than 3 order of magnitude in frequencies.
- We first fitted with log – parabolic (LP) model (left panel). The fits were poor.
- We then fitted with log – parabolic (LP) + Power Law (PL) → (LPPL) model which show significant improvement.
- These models indicate that the optical/UV and X-ray flux variations are mainly driven by model normalization, but the X-ray band flux is also affected by spectral variations, as parameterized with the model curvature parameter.
- The energy at which the emitted power is maximum correlates positively with the total flux. As spectrum shifts to higher frequencies, the spectral curvature increases.

Bhagwan, Gupta, Papadakis, Wiita, 2014, MNRAS, 444, 3647

Project 3.

QPOs in Blazars

Presence of QPOs are fairly common in micro-quasars but rare in AGN

Galactic Black Hole Binary (GRB) Cartoon

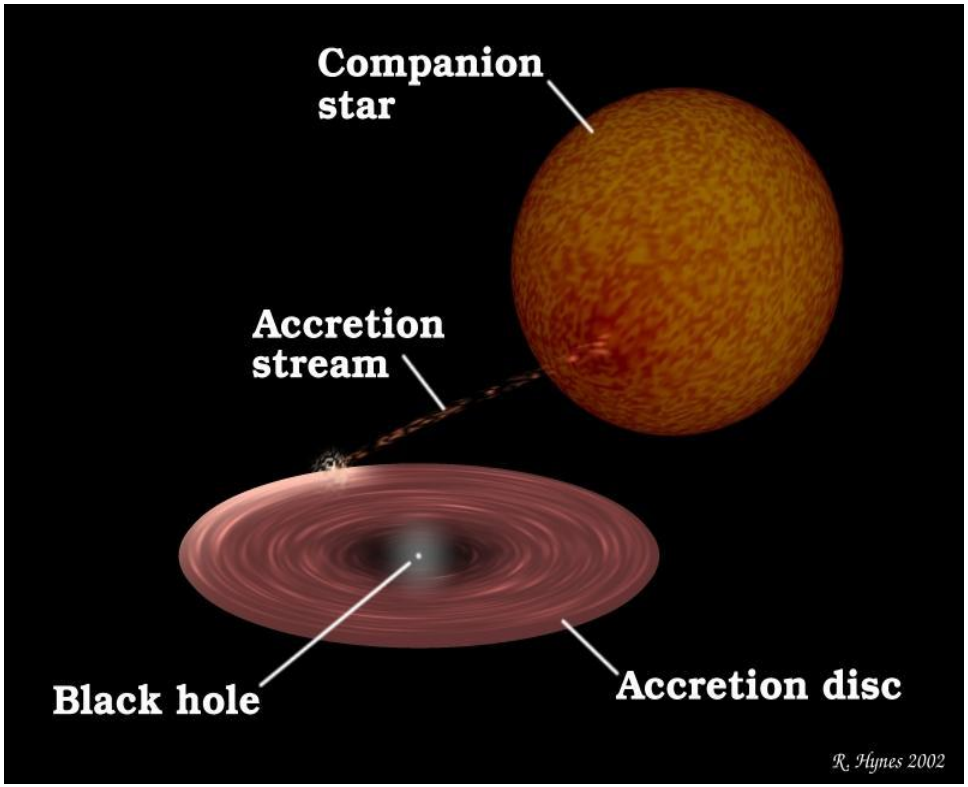

Active Galactic Nuclei (AGN) Cartoon

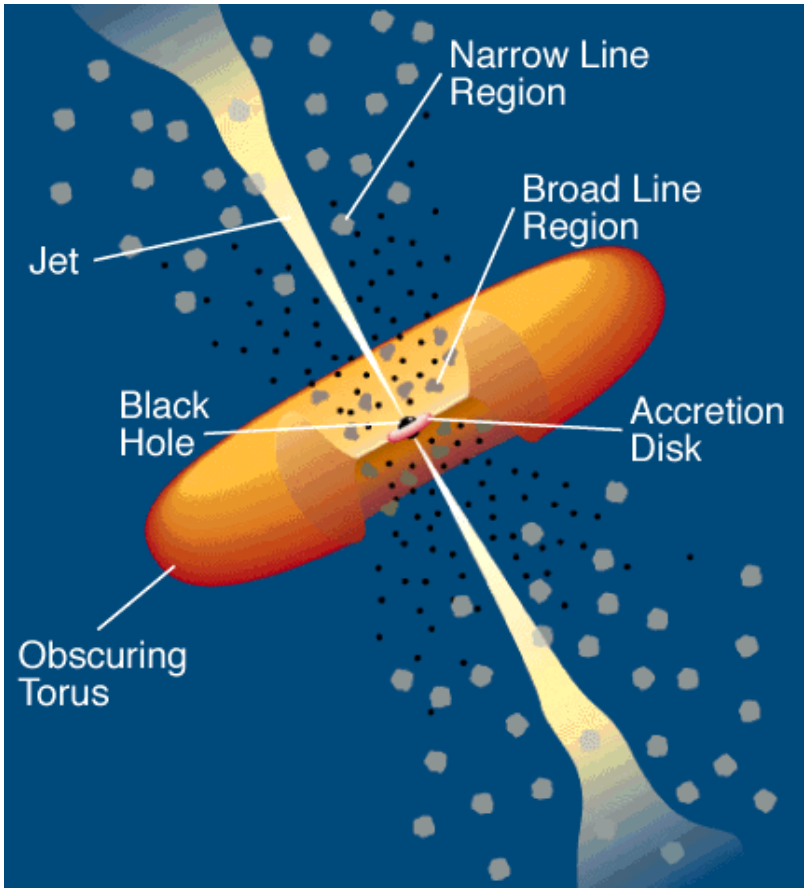

Hot spot on accretion disk can possibly explain QPO on IDV timescale but this model is ruled out for STV & LTV timescales because BH mass exceeded 10^10 M_sun

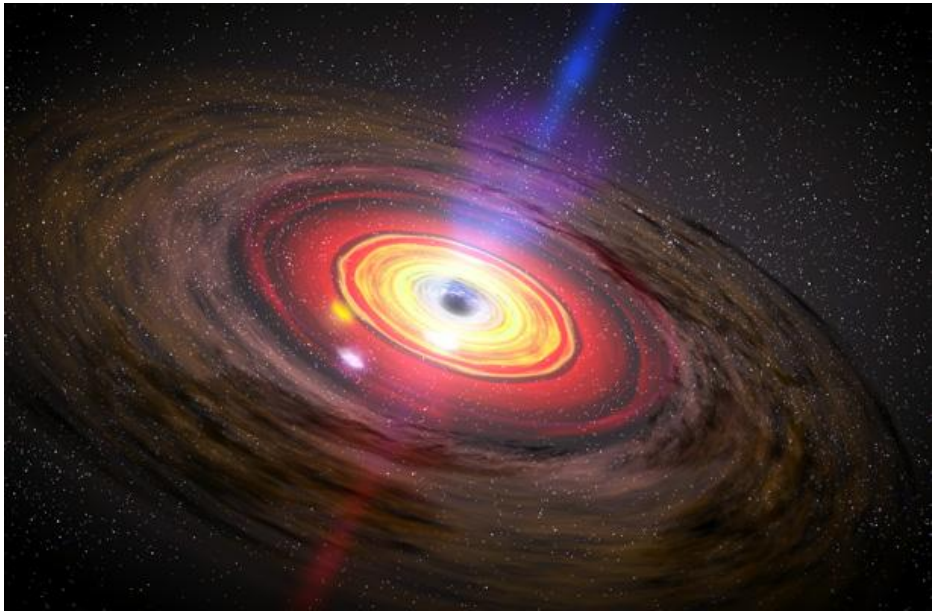

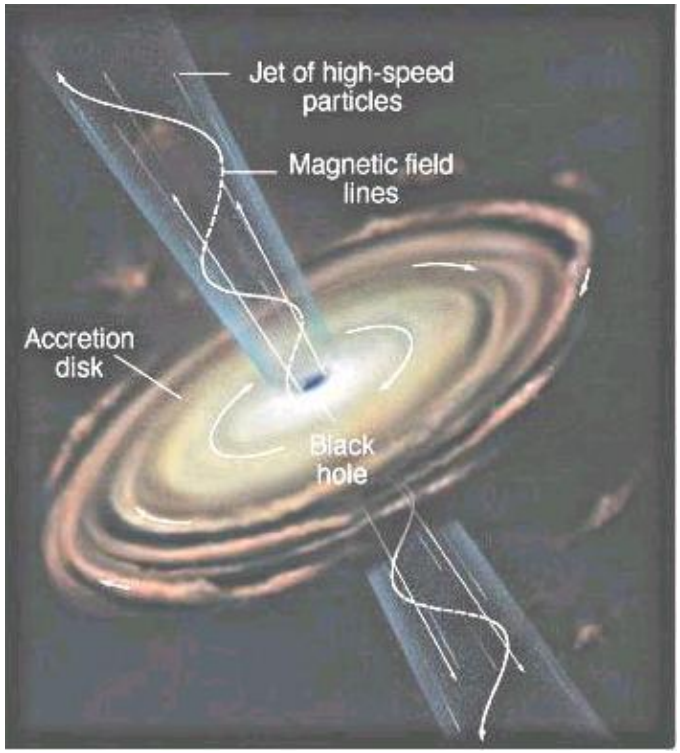

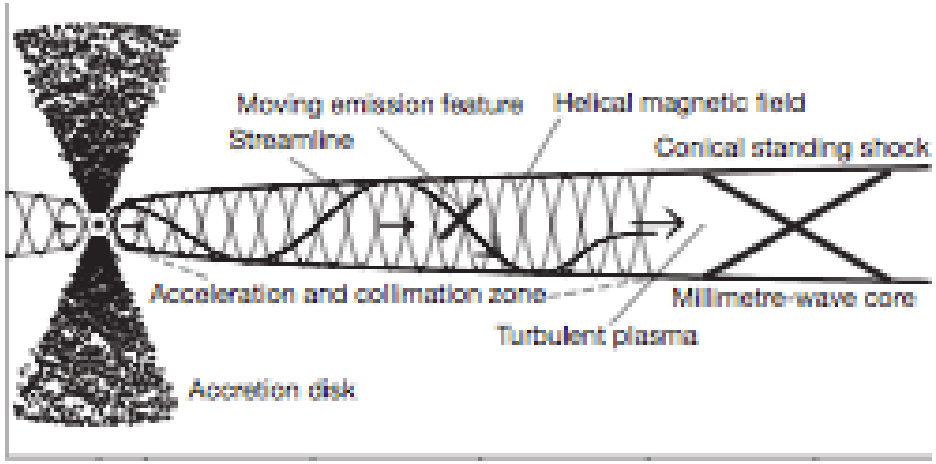

Jet propelled by B-fields twisted by BH Accretion disk

Our Results

EM Band	QPO Results	Time Scale	Methods	Ref.
optical	QPO in S5 0716+714 on 5 occasions	25 to 73 min.	wavelet	**ACG**, AKS, PJW, **ApJ, 690**, 216 (2009)
X-ray	QPO in AO 0235+164 QPO in 1ES 2321+419	17 days 420 days	SF, DCF, LSP, Data Folding	BR, PJW, **ACG**, **ApJ, 696**, 2170 (2009)
X-ray	**QPO in PKS 2155-304**	**4.6 hour**	**SF, wavelet, PSD, MHAoV, data folding**	PL, **ACG**, HG, PJW, **A&A Lett. 506**, L17 (2009)
X-ray	Hint of QPO in ON 231 Hint of QPO in PKS 2155-304	3.3 hour 1.9 hour	SF, PSD	HG, **ACG**, PJW, **ApJ, 718**, 279 (2010)
optical	**QPO in S5 0716+714** **Fastest QPO ever detected in any AGN**	**15 min**	**SF, PSD, LSP, data folding**	BR, **ACG**, UCJ, SG, PJW, **ApJL, 719**, L153 (2010)
optical	**Weak QPO in S5 0716+714**	**1.1 days**	**SF, PSD, wavelet, MHAoV, data folding**	**ACG**, et al. (34 authors) **MNRAS, 425**, 2625 (2012)

Black Hole Mass Estimation with Periodic or QPO Timescale

Causality argument gives the size of emitting region R <= c delta T (obs). Minimum size of such an emitting region is fairly closely related to the gravitational radius of BH,

$$R \geqslant R_g \equiv GM/c^2 \text{ (e.g., Wiita 1985)}$$

The minimum likely period corresponds to the orbital period at the inner edge of the accretion disk, which is usually is given by marginally stable orbit, R_{ms}

For a non rotating (Schwarzschild) BH

$$R_{\rm ms} = 6GM/c^2 = 6R_g$$

a maximal Kerr BH, with angular momentum parameter $a \to 1$, $R_{\rm ms} \to R_g$. However, for a more realistic maximum angular momentum parameter of $a = 0.9982$ then $R_{\rm ms} \simeq 1.2R_g$ (e.g., Espaillat et al. 2008).

The angular velocity of co-rotating matter orbiting a BH, as measured by an inertial observer at infinity, is given by (e.g., Lightman et al. 1975)

$$\Omega = \frac{M^{1/2}}{r^{3/2} + aM^{1/2}}, \tag{3}$$

where geometrical units, $G = c = 1$, have been used, and $r = R/R_g$. This leads to an expression for the BH mass in terms of the observed period, P, in seconds,

$$\frac{M}{M_\odot} = \frac{3.23 \times 10^4 P}{(r^{3/2} + a)(1 + z)}. \tag{4}$$

The nominal masses obtained in this fashion for a Schwarzschild BH (with $r = 6$ and $a = 0$) are in Column 7 of Table 1, and those obtained for a maximal Kerr BH (with $r = 1.2$ and $a = 0.9982$) are in Column 8. If the periodic perturbations in the

XMM-Newton data of PKS 2155-304

4.6 hour QPO & 3.8 cycles

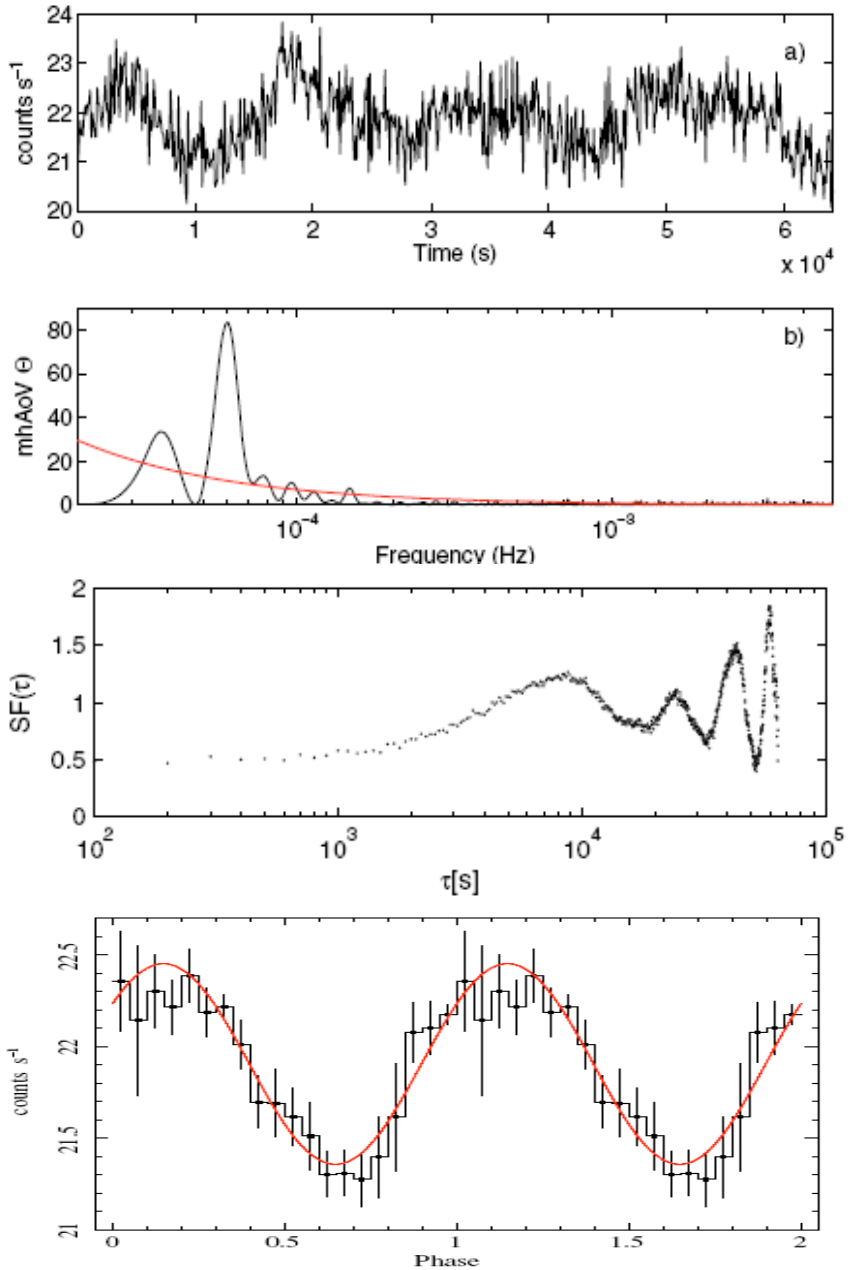

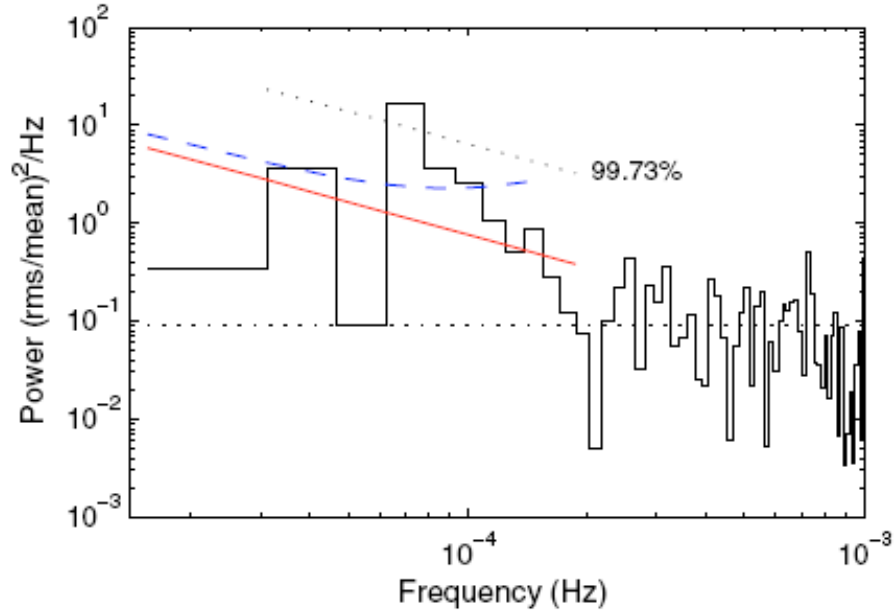

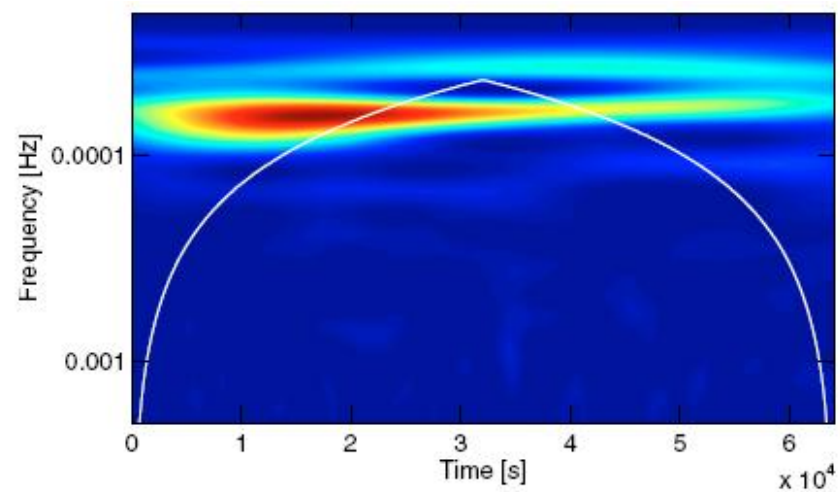

Lachowicz, **Gupta**, Gaur, Wiita, 2009, A&A Lett., **506**, L17

The simplest of these models for BHs would attribute the quasi-periods to particularly strong orbiting hotspots on the disks at, or close to, the innermost stable circular orbit allowed by general relativity (e.g., Abramowicz et al. 1991; Mangalam & Wiita 1993). If such simple models apply in this case, and the QPO is indeed real, then we would estimate the BH mass for PKS 2155−304 to be 3.29×10^7 *M* (Sun) for a non-rotating BH and 2.09×10^8 *M* (Sun) for a maximally rotating BH.

A shock propagating down a jet which contains quasi-helical structures, whether in electron density or magnetic field, can produce a QPO, with successive peaks seen each time the shock meets another twist of the helix at the angle that provides the maximum boosting for the observer (e.g., Camenzind & Krockenberger 1992). Instabilities in jets just might be able to excite such helical modes capable of yielding fluctuations that are observed to occur on the time-scale seen in PKS 2155−304 (e.g., Romero 1995). Or they could arise as the jet plasma is launched in the vicinity of SMBH and thus actually originate in the accretion flow but become amplified in the jet. Another very plausible origin for a short-lived QPO would be turbulence behind the shock in the relativistic jet (e.g. Marscher et al. 1992), as again intrinsically modest fluctuations could be Doppler boosted.

Summary

- Multi-wavelength Flux Variability is detected in blazars on diverse timescales.
- On STV and LTV timescales, in general BL Lacs show BWB while FSRQ show RWB trend.
- In BL Lacerate, we noticed optical flux and polarization are anti-correlated.
- In a single LC of HBL PKS 2155 – 304, we noticed stable flux, QPO, decline flux and flaring state.
- In LTV LCs, optical and UV LCs were correlated, and soft and hard X-ray LCs were correlated in PKS 2155 – 304 and 3C 273.
- Optical to X-ray SEDs are well fitted by PLLP model in PKS 2155 – 304
- In 3C 273 and PKS 2155-304 we found, synchrotron cooling and particle acceleration are at work on different epoch of observations.
- Spectral variability is seen in blazars in XMM-Newton and NuStar observations.
- QPOs in Blazars are rare but occasionally detected on diverse timescales.

Acknowledgement to following students and collaborators for the collaborative work.

Ph.D. Students: Haritma Gaur, Jai Bhagwan, Aditi Agarwal, Nibedita Kalita, Ashwani Pandey, Vishi Aggrawal

Collaborators: P. J. Wiita, I. E. Papadakis, P. Lachowicz, R. Bachev, M. Uemura, J. H. Fan, O. Kurtanidze, and about 30 other collaborators worldwide.

THANKS